NRL Report 6934

Study of Doppler Spectra of Radar Sea-Echo

G. R. VALENZUELA AND M. B. LAING

Wave Propagation Branch
Electronics Division

November 3, 1969

NAVAL RESEARCH LABORATORY
Washington, D.C.

CONTENTS

Abstract	ii
Problem Status	ii
Authorization	ii
INTRODUCTION	1
SCATTERING MODELS	2
EXPERIMENTAL RESULTS	5
Bandwidth of Radar Sea-Echo as a Function of Sea-State	6
Doppler Frequency of Radar Sea-Echo	10
DISCUSSION AND CONCLUSIONS	11
ACKNOWLEDGMENTS	14
REFERENCES	14
APPENDIX A — Parameters of the Four-Frequency Radar System	16
APPENDIX B — Sea Conditions and Pertinent Information	19
APPENDIX C — Partial Collection of Spectra	23

ABSTRACT

Doppler spectra of radar sea-echo were investigated theoretically and experimentally. Electromagnetic scattering models were developed with composite rough surfaces, i.e., Bragg resonant water waves superimposed on a carrier water wave; and basic concepts in hydrodynamics were developed for a gravity wave of finite height. The ideas are carried over to the sea, where the assumption of a fully developed sea yields wave height expressions of the form $\sim H^{0.4 \text{ to } 0.6}$ for the width of the spectra of radar sea-echo, H being the height of the carrier water wave. The simple models yield the order of magnitude and the wave height dependence of the spectra width, but they fail to give its observed polarization dependence.

New experimental results on spectra of radar sea-echo from the Four-Frequency Radar (428 MHz, 1228 MHz, 4455 MHz, and 8910 MHz), for sea conditions which ranged from 1 to 2 ft waves and 1 to 2 knot winds to 26-ft waves and 46 to 48 knot winds, show that the bandwidth of radar sea-echo is polarization and frequency dependent, and the differential doppler, between horizontal and vertical polarization, is frequency and depression angle dependent. Both the "noisiness" of the spectra and the greater spectral width of the horizontal return indicate spray over the sea might be the mechanism responsible for the dependencies observed.

PROBLEM STATUS

This is an interim report on this problem

AUTHORIZATION

NRL Problem R02-37
Project A31-533/65269R008 01-02

Manuscript submitted May 15, 1969.

STUDY OF DOPPLER SPECTRA OF RADAR SEA-ECHO

INTRODUCTION

During the past years the scattering mechanism responsible for radar sea-clutter has been investigated in great detail. As a consequence, with the advent of recent developments in slightly rough and composite surface scattering theories [1-5], the problem of modeling the properties of average radar backscattering cross sections seems to be well under control.

To further improve the sea-clutter model it is desirable to have additional information on doppler spectra of radar sea-echo to gain new perspectives on the electromagnetic scattering processes from a moving air-sea boundary. A review of previous work on doppler shows that Crombie [6], in 1955 at 13.56 MHz, observed that the mean doppler frequency of radar sea-echo corresponded to the phase velocity of water waves which satisfied the Bragg resonant condition [7], i.e., water waves of wavelength half the radar wavelength, for grazing incidence. In 1958 Ament et al. [8], with a horizontally polarized radar at 220 MHz, noted that the width of doppler spectra of sea-echo was comparable to the width of the distribution of velocity obtained from the complete energy spectral density of the water waves on the surface, indicating that in addition to the resonant scatterers, other water waves make a significant contribution. Hicks et al. [9], from the University of Illinois, using horizontally polarized X-band, concluded that radar return was produced by two types of scatterers, one set made by "unbroken" water, of dimension one-half the wavelength of the radar frequency, moving at the orbital velocity (fluid velocity) of the gravity waves of maximum amplitude, and a second set made by wind-blown spray. The half-power width of the spectra, as a function of sea conditions, followed the empirical expression 11 H_s / T_m, where H_s is the average of the third highest waves (significant wave height) and T_m is the period of the gravity wave of maximum amplitude. Recently Pidgeon [10], with dual polarized C-band coherent radar, for grazing angles of 0.3 to 8 degrees, found that the frequency at which the spectra had the maximum amplitude was polarization dependent, with the doppler spectra for horizontal polarization having the maximum amplitude at a higher frequency than the vertical polarization.

The observations at 220 MHz and higher indicate a composite type of surface producing the scattering, i.e., resonant water waves superimposed on gravity waves or swells. Consequently, in the sea, the transition from a purely slightly rough surface to a composite rough surface (electromagnetically) must occur somewhere between 13.56 MHz and 220 MHz.

The composite surface model has already been used successfully to explain polarization effects in radar backscattering cross-section experiments [4,5], and its applicability to doppler effects will now be explored.

Using basic concepts in hydrodynamics to develop composite surface scattering models for gravity waves of finite height, the order of magnitude of orbital motion effects that might be expected in the spectra of radar sea-echo will be estimated. Finally, new experimental results will be presented on doppler spectra obtained from the phase channel of the four-frequency radar of the Naval Research Laboratory, both to verify the models and show that the sea-clutter process is much more complex than the earlier experiments at single frequencies have suggested. The simple models account only for

orbital motion effects in the spectra, while other mechanisms seem to be significant in the spectra for horizontal polarization.

SCATTERING MODELS

Some basic concepts in classical hydrodynamics will be introduced first in order to formulate the scattering models. In the sense of the Stokes expansion, the dynamics of a water wave of finite height can be derived from the dynamics of a sinusoidal water profile [11] (Fig. 1)

$$\zeta(\mathbf{x}, t) = a \cos \chi \tag{1}$$

to which corresponds a velocity potential (infinite depth)

$$\phi(\mathbf{x}, t) = \omega a k^{-1} e^{kz} \sin \chi , \tag{2}$$

where ω is the angular velocity of the water wave, k the wave number of the water wave, and $\chi = \mathbf{k} \cdot \mathbf{x} - \omega t$ the phase factor.

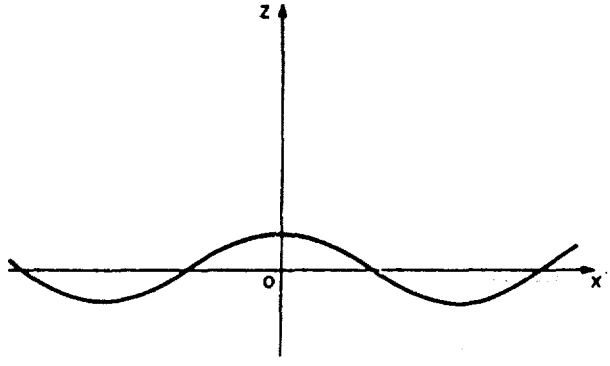

Fig. 1 - Sinusoidal water wave profile

To the first order of the wave amplitude a, the velocity components, $u_t^{(1)}$ and $w_t^{(1)}$ (Lagrangian description) are identical to the Eulerian velocity components, dx/dt and dz/dt:

$$dx/dt = \partial\phi/\partial x = u_t^{(1)} = \omega a e^{kz} \cos \chi , \tag{3a}$$

$$dz/dt = \partial\phi/\partial z = w_t^{(1)} = \omega a e^{kz} \sin \chi . \tag{3b}$$

Carrying Phillips procedure to the second order, the fluid velocity can be shown to be

$$u_t = u_t^{(1)} + u_t^{(2)} = \omega a e^{kz} \cos \chi + \omega a^2 k e^{2kz} , \tag{4a}$$

$$w_t = w_t^{(1)} + w_t^{(2)} = \omega a e^{kz} \sin \chi . \tag{4b}$$

To the first order the fluid describes circles, and to the second order a drift velocity appears in the horizontal component. Kinsman [12] has shown that in the Stokes procedure

of the surface profile, $z = \zeta$ is no longer sinusoidal but to the third order tends toward a trochoid. Thus, a trochoical wave profile could be used together with Eq. (4) for the fluid velocity components to model a gravity wave in the sea. Such a model must be approximate, since the Stokes expansion has been shown to have a zero radius of convergence and the Gerstner wave, which has a pure trochoidal shape, assumes zero drift, which is not true in the sea. Kinsman [13] notes that in the sea the waves have properties of both Stokes and Gerstner wave.* The local slope for a trochoidal profile is given by

$$\partial\zeta/\partial x = -ak \sin X/(1 - ak \cos X) , \tag{5}$$

which for waves of infinitesimal amplitude is the same as for a sinusoidal profile.

A deterministic type of composite scattering surface can be constructed using a long-crested carrier water wave of the type described and on which Bragg resonant water waves, moving at the fluid velocity of the carrier wave, are superimposed. For simplicity, it will be assumed that there is no interaction between the scatterers and the carrier wave, and the scatterers have constant amplitude throughout. A radar illuminating such a surface (Fig. 2) at a depression angle γ will observe a doppler shift because of the component of fluid velocity v_R given by

$$v_R = \omega a e^{kz} \cos (X + \gamma) + \omega a^2 k e^{2kz} \cos \gamma . \tag{6}$$

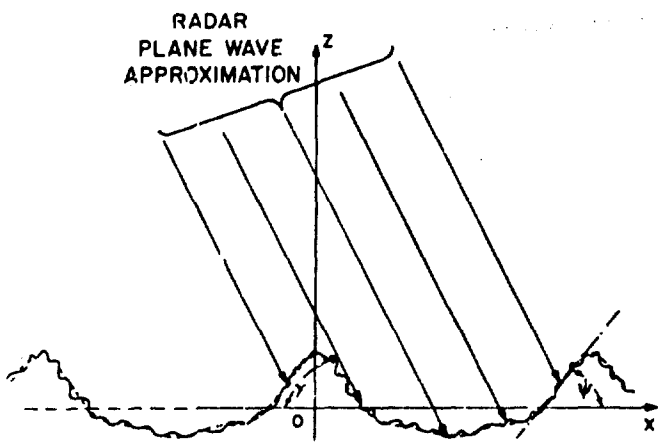

Fig. 2 - Geometry of radar scattering from a deterministic long-crested composite surface

Doppler spectra can be calculated by weighting the amplitude of a spectra of velocities, Eq. (6), according to the backscattering cross section given by slightly-rough theory, according to the local angle of incidence of the electromagnetic wave to the water wave [3]. Doppler spectra calculated by this procedure have yielded broader spectra for vertical polarization than for horizontal polarization, while measurements show the converse is true. The effect of "tilts" in the backscattering cross section [4,5] would increase the bandwidth for the horizontal spectra, and in the limit it is reasonable to assume that this deterministic composite scattering model would yield the same bandwidth

*It is not essential to use the trochoidal profile, but for a given wave height and period the trochoid has greater slopes.

for both polarizations. Thus, this model could not account for the polarization dependence of the spectral bandwidth of radar sea-echo. However, it does give the bandwidth of the spectra, and the wave height dependence, and their order of magnitude. This composite surface model will now be carried over to a surface like the sea.

The sea is made up of a continuum of water waves. Oceanographers have found that as a first approximation, the sea can be considered a Gaussian random moving surface. Longuet-Higgins [14] derived many statistical properties for such a surface, among them the probability density function for the velocity of the zeros and specular points (points on the face of a surface with a given slope). The velocity of the zeros is equivalent to the Eulerian velocity for a single water wave, to the first order this velocity can be taken as the particle or fluid velocity. Longuet-Higgins's probability density function $p(v)$ for the velocity of the zeros and the specular points is

$$p(v) = \frac{1}{2} \frac{\nu^2}{[(v - \bar{v})^2 + \nu^2]^{3/2}} , \tag{7}$$

where $\bar{v}$ is the mean velocity of the fluid and ν^2 relates to moments of the water waves spectrum. For a narrow band type of spectrum, carrier water wave plus secondary water waves equivalent to a composite type scattering surface, ν^2 in both distributions simplifies to

$$\nu^2 = \left(\frac{\mu_{20}}{\mu_{00}}\right)\left(\frac{\bar{v} - \Gamma}{\bar{k}}\right)^2 , \tag{8}$$

where μ_{20} is the variance of surface slopes, μ_{00} the variance of surface heights, $\bar{v}$ the phase velocity of the carrier wave, $\bar{k}$ the wave number of the carrier wave, and Γ the group velocity $(\partial\omega/\partial k)$. For a gravity wave, $\Gamma = \bar{v}/2$. The probability density function for the velocity of the zeros can be taken as an approximation to the doppler spectra. It is not possible to account explicitly for any scattering amplitude weighting in this approach.

In an alternative manner an average fluid velocity on the sea can be calculated directly. Recalling from Eq. (3) that the classical expression for orbital motion is $v_f^2 = u_f^2 + w_f^2 = \omega^2 a^2 e^{2kz}$ for a mean level $z = 0$, it can be averaged in wave number space using the energy spectral density of the surface, $W(k)$.* Bye [15] obtained drift velocity in the sea using a similar method. The averaging is performed in the following manner: since the variance of height $\overline{a^2}$ is related to the area under the spectrum,

$$\overline{a^2} = \int W(\mathbf{k})\, k\, dk , \tag{9}$$

orbital motion $\omega^2 a^2$ is obtained from

$$\overline{v_f^2} = \int \omega^2 W(k)\, k\, dk , \tag{10}$$

a type of scalar average in which phases and directions of waves are not included, and where for gravity waves $\omega^2 = gk$.

In Eq. (10) the energy spectrum for the waves in the sea is needed, and for convenience the spectrum for a fully developed sea will be used. There are various expressions

*This method was suggested by Dr. J. W. Wright of the Naval Research Laboratory in private communication.

for the "equilibrium" range for the energy spectrum for a fully developed sea [16,17]. These spectra are of the form

$$W(\mathbf{k}) \propto B\, k^{-\alpha} , \tag{11}$$

where α varies from 3.75 to 4.5 and the constant B varies from 2.5×10^{-3} to 7.5×10^{-3}.

In calculating orbital velocity the lower and upper limits in the integration will be taken to be gU^{-2} and $\beta \cos\gamma$, where g is the acceleration of gravity, U the wind speed, $\beta = 2\pi/\lambda$ the radar propagation constant, and γ the radar depression angle.

The orbital velocity, Eq. (10), obtained for the different spectra is of the form

$$\overline{v_\ell^2} \propto C'(\overline{a^2})^{3/7-3/5} , \tag{12}$$

where the constant C' and the range of the exponent shown depends on the spectrum used. Equation (12), an important result, shows the wave height dependence of orbital velocity. The width of the radar spectral return, in units of velocity, should be of the order of $2(\overline{v_\ell^2})^{1/2}$. Surprisingly enough, if the fully developed sea assumption is used in both the deterministic model and Longuet-Higgins density function, we obtain a similar wave height dependence as Eq. (12), except the value for the constant depends on the model used.

The exact value of the constant can be obtained if the boundary value problem of the electromagnetic radiation scattered by the air-sea interface is solved, or from experimental results.

EXPERIMENTAL RESULTS

Doppler spectra have been obtained from the phase data of the Four-Frequency Radar (4FR) of the Naval Research Laboratory. The complete system has been described in great detail by Guinard et al. [18], thus only a description of whatever is necessary to clarify our analyses will be included here. The 4FR is a phase coherent pulse radar which is capable of measuring the elements of the scattering matrix of the radar return at 428 MHz (P-band), 1228 MHz (L-band), 4455 MHz (C-band), and 8910 MHz (X-band) (Appendix A). One of the two output channels of the 4FR is a pulse-to-pulse sample of the cosine of the phase of the clutter return. Doppler spectra can be obtained from the phase data by the cosine Fourier transform of the correlation function of the samples, or by finding directly the power spectral estimates within a frequency interval by a Fourier analysis of the record. The second method was used since it gave added flexibility, in that degrees of freedom, frequency resolution, and length of record could be separated. The resultant spectrum calculated from the phase data of the radar return from an airborne system is the convolution of the so-called platform motion spectrum and the sea-echo spectrum. The platform motion spectrum has a mean doppler frequency, f_D, given by the well known expression for an along-track-looking radar

$$f_D = \frac{2v_g}{\lambda} \cos\gamma , \tag{13}$$

where v_g is the ground speed and λ the radar wavelength. In general, the doppler frequencies for the L, C, and X bands are greater than the radar pulse repetition frequency f_{PRF}, and thus the spectra appear at frequency centers (aliases) f_{cn}, given by

$$f_{cn} = f_D \pm n\, f_{PRF} . \tag{14}$$

where n is an integer. If the spectra at the aliases appear "unfolded" within zero frequency and $f_{PRF}/2$ after detection, the spectra at the aliases are exact replicas of the true spectra.

Also, because of the aircraft motion, at least two mechanisms act to broaden the resultant spectra and contaminate the intrinsic spectra of sea-echo. These are (a) platform motion (azimuthal and elevation contributions), and (b) decorrelation because of relative motion and finite resolution cell.

a. Platform motion — Because the radar resolution cell on the sea is finite, and the ground speed varies throughout the resolution cell, the resultant spectrum is broadened. To estimate the magnitude of this broadening, Ridenour's [19] expressions for an along-track-looking radar will be used; they are:

$$\Delta v_e = \frac{1}{2} \frac{v_g c\tau}{h} \sin^2 \gamma \tan \gamma \tag{15}$$

and

$$\Delta v_a = \frac{1}{8} v_g (\Delta\Theta)^2 \cos \gamma \, . \tag{16}$$

where c is the velocity of light in vacuo, τ the radar pulse width, h the aircraft altitude, $\Delta\Theta$ the azimuthal antenna beamwidth (half-power), and γ the depression angle.

b. Decorrelation because of relative motion and finite resolution cell — This mechanism was discussed by Barrick [20] and appears because from one pulse to the next the resolution cell slides along the ground or sea and cells for two adjacent pulses overlap only partially, introducing a decorrelation of the scatterers responsible for the scattering. The correlation of overlapping scatterers in a pulse-to-pulse basis decreases linearly as a function of aircraft velocity and time. The Fourier transform of such a correlation function gives a spectrum which has an approximate half-power width Δv_m (velocity units) of

$$\Delta v_m \approx \frac{\lambda v_g \cos \gamma}{c\tau} \, . \tag{17}$$

Of course, atmospheric turbulence will also affect the aircraft velocity and attitude. The antenna mount was a gyro-controlled stabilization system, and long-term attitude perturbations should be completely canceled, but without an independent measurement of short time perturbations it is not possible to separate their magnitude from statistical fluctuations.

To calculate the total broadening because of the aircraft motion, assumptions of independence between the different mechanisms and Gaussian shaped spectra have been made. Thus, the total broadening Δv can be calculated from

$$\Delta v = [(\Delta v_e)^2 + (\Delta v_a)^2 + (\Delta v_m)^2]^{1/2} \, . \tag{18}$$

At grazing incidence P-Band has the largest broadening and with increasing depression angle all trequency bands attain the same broadening, Figure 3.

Bandwidth of Radar Sea-Echo as a Function of Sea-State

Using the assumptions of independence and that the shape of the component spectra are Gaussian, the nondesirable broadening can be removed if its magnitude is small

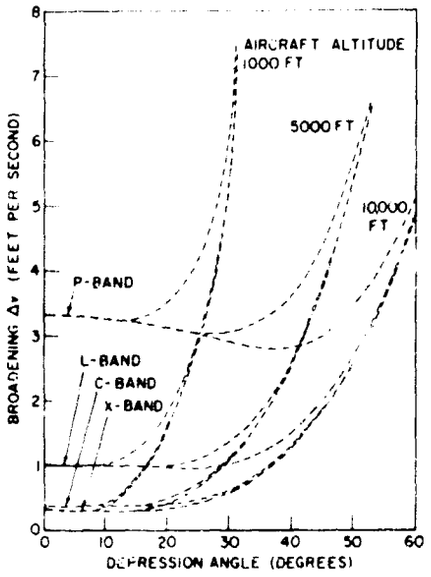

Fig. 3 - Total broadening in doppler spectra because of aircraft motion and finite resolution cell (aircraft velocity: 300 ft/sec, radar pulse width: 0.25 μsec)

compared to the sea-clutter spectral width. To estimate the aircraft's velocity, the mean doppler frequency from the P-band spectra, which is unambiguous, has been used. Any orbital motion shift will be small compared to the aircraft's velocity.

In Appendix B the sea conditions in which the data were taken and also other information pertinent to the spectra calculations are presented. In Appendix C a partial collection of the radar spectra used to obtain the data has been compiled.

In Figs. 4 and 5 the spectra as a function of wave height for the C-band, vertical and horizontal polarizations, are shown. In the figures the first letter in VV, HH, HV, and VH stands for the polarization of the transmitted signal, and the second letter stands for the polarization of the received signal, where V stands for vertical and H for horizontal.

In analyzing the doppler spectra, their half-power width was measured directly from the graphs. An actual calculation of the spectral variance to estimate width was abandoned because a direct measurement seemed to be a fairer estimate of the actual spectral width for the type of data analyzed. The measured spectral widths were corrected by subtracting the square of Eq. (18) from the square of the measured widths.

The broken line in Fig. 6 is added to show the wave height dependence $H^{1/2}$ on orbital velocity, in agreement with Eq. (12). The constant was selected arbitrarily to fit the data; however, the scattering models predict the constant to be anywhere between 1 and 4.

In Fig. 7 the points obtained for all the radar frequencies have been included. For 1 to 2 ft waves the P-band data are absent because platform motion was too large to be removed.

Note that the width for the horizontal spectra is broader than the spectra for vertical polarization. Hicks et al. concluded that the width for the horizontal spectra was greater than that estimated from orbital motion alone. Here in agreement with Pidgeon, we conclude that the spectra for vertical polarization seem to be attributable to orbital motion alone, while the horizontal spectra are broader and noisier, and should be attributed to orbital motion and wind-blown spray at the air-sea boundary.

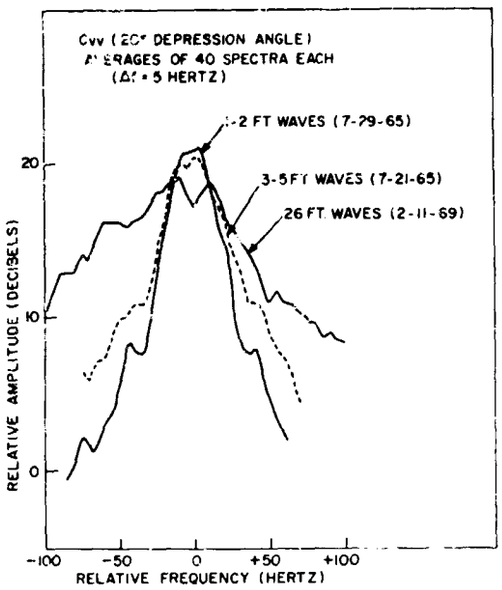

Fig. 4 - Doppler spectra of radar sea-echo broadening because of sea wave height (C-band, vertical polarization)

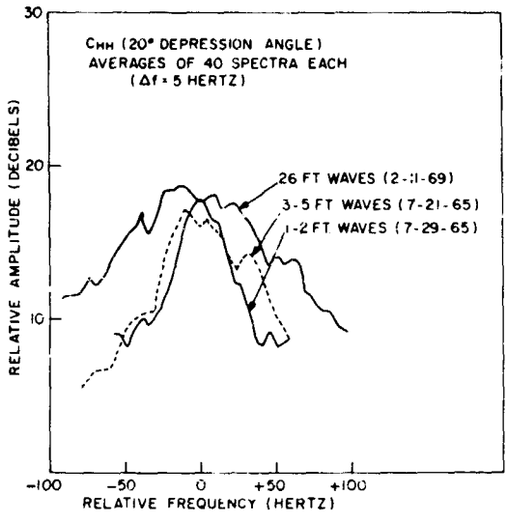

Fig. 5 - Doppler spectra of radar sea-echo broadening because of sea wave height (C-band, horizontal polarization)

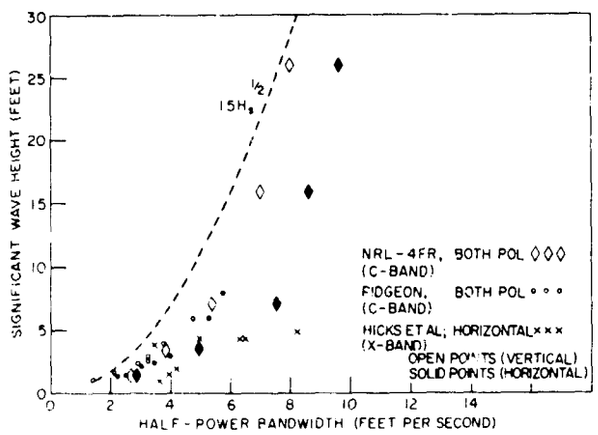

Fig. 6 - Half-power bandwidth of radar sea-echo spectra as a function of significant wave height of the sea (C-band)

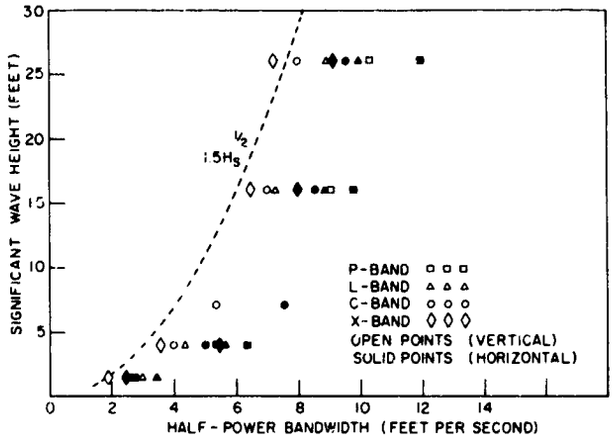

Fig. 7 - Summary of corrected half-power bandwidth of radar sea-echo spectra from the NRL 4FR as a function of significant wave height of the sea (points are averages over depression angles between 5 and 30 degrees)

Another effect apparent in the data is that the width of the spectra decreases with increasing radar frequency; this is surprising, since the converse seems to be much more reasonable at first. However, thinking in terms of the composite surface scattering model, the effective rms slope of the carrier wave for the P-band should be smaller than that for the higher frequencies. Thus, all velocities on the surface would have a near-constant amplitude weight for these, with the net result of a broader spectra. For calm sea condition, 1 to 2 ft waves, the frequency dependence was weaker than in Fig. 8 (close to unity) for all frequencies except the X-band, which had a similar dependence to that shown in the figure. The bandwidth of the spectra for vertical polarization seems to be independent of depression angle for angles between 5 and 30 degrees.

Another possibility for the broader spectra at the lower radar frequencies is the longer length of data required to have a smaller frequency resolution (Table B3, Appendix B); any perturbation in the aircraft velocity would be much more evident in the spectra for these lower frequencies. However, the L and C-bands both use the same length of data and the spectra for the lower frequency are still broader.

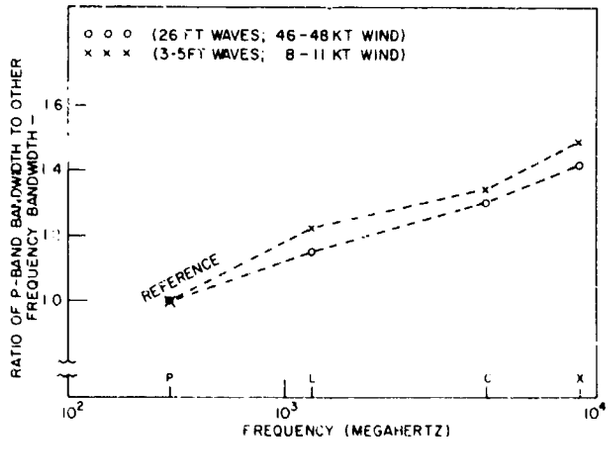

Fig. 8 - Corrected half-power bandwidth of radar sea-echo spectra as a function of radar frequency (vertical polarization)

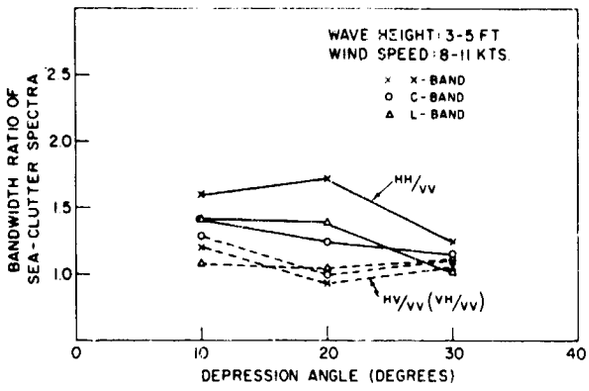

Fig. 9 - Polarization dependence of the half-power bandwidth of radar sea-echo spectra (21 July 1965)

In Fig. 9, data from 21 July 1965, show the ratio of bandwidth for horizontal polarization (HH) to that of vertical polarization (VV) decreasing with depression angle. The ratio of the bandwidth for the crosspolarized spectra to that of the vertically polarized spectra is smaller than the previous ratio. Both of these ratios seem to be frequency dependent. In Fig. 10 the bandwidth for horizontally polarized spectra as a function of depression angle is shown explicitly.

Doppler Frequency of Radar Sea-Echo

Although the bandwidth of the spectra of radar sea-echo could not be obtained directly and certain assumptions were necessary to recover it, the differential doppler between the various spectra is more exact.

The averages for the differential doppler as a function of wind speed in the C and X bands follow the general trend found by Pidgeon (Fig. 11). The important fact found here is that the differential doppler is frequency dependent as shown by the figure. No

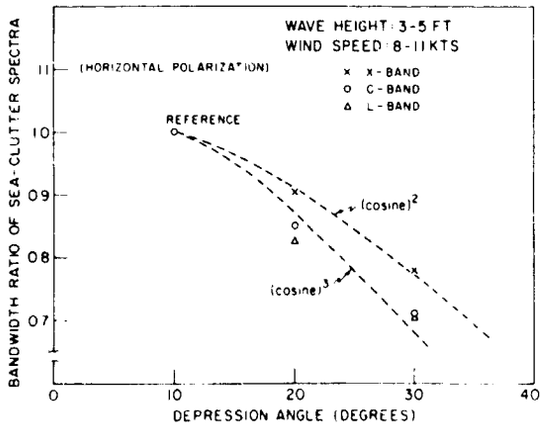

Fig. 10 - Half-power bandwidth of radar sea-echo spectra as a function of depression angle (horizontal polarization)

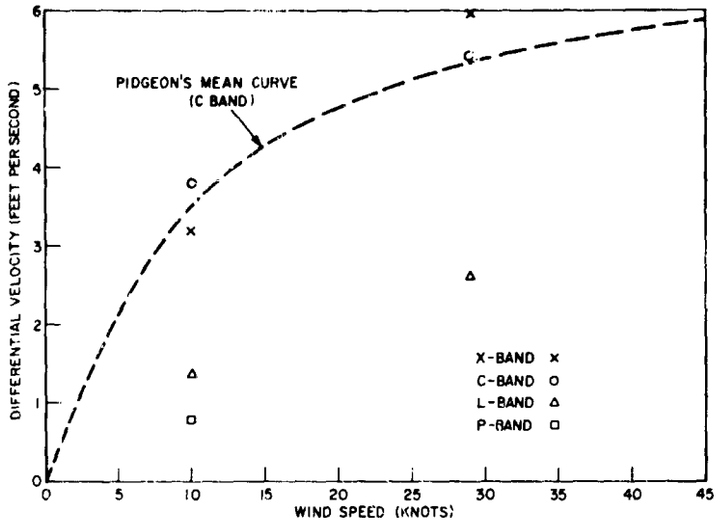

Fig. 11 - Average differential velocity of radar sea-echo spectra (between spectra for HH and VV polarizations) as a function of wind speed, for depression angles smaller than 10 degrees

conclusive trend was found in the data for the days 29 July 1965 and 11 February 1969. The differential doppler between VH and VV was small for small winds and increased with wind speed, but its magnitude was still smaller than that between (HH and VV). As expected, no noticeable differential doppler was observed between VH and HV for all wind speeds (reciprocity).

DISCUSSIONS AND CONCLUSIONS

The experimental results on doppler spectra of radar sea-echo from the 4FR show that the mechanisms responsible for sea-clutter are quite complex. In particular, the measurements show that several of the parameters of the spectra are frequency and depression angle dependent.

The simple scattering models developed in terms of composite surfaces seem to be most applicable to the spectra observed for vertical polarization. For example, the measured bandwidth of the spectra has a wave height dependence similar to that obtained from the models, and it is independent of radar depression angles between 5 and 30 degrees, which is expected from the models.

In the experimental results, the spectra for horizontal polarization are broader than those for vertical polarization, while the scattering models based on purely orbital motion predict the converse. By allowing for "tilt" effects in the backscattering cross section [4,5], composite surface models at most will yield the same bandwidth for the spectra for both polarizations. A broader spectra for horizontal polarization cannot be accounted for from purely orbital motion effects; thus there must be an additional mechanism contributing. Several characteristics of the spectra seem to indicate that spray over the water might be responsible for the broadening, e.g., the noisy appearance of the spectra for horizontal polarization, similar to the general appearance of spectra when rain is present, and the frequency dependence of the magnitude of the differential doppler between HH and VV.

To account for the width of the spectra for horizontal polarization, the scattering of electromagnetic waves from an air-spray-sea interface should be investigated. As there is very little quantitative work published on spray on the sea, this is an area in which a basic study might be fruitful.

In Fig. 12 the differential velocity, as a function of depression angle, is shown. This is the first time that a variation of differential velocity with depression angle has been obtained. To arrive at a more definite trend, additional measurements in this area would be desirable.

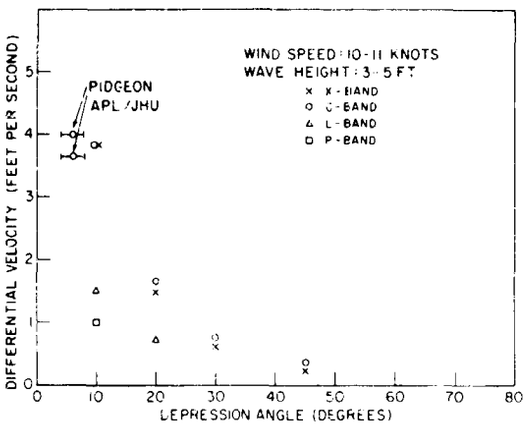

Fig. 12 - Average differential velocity of radar sea-echo spectra (between spectra for HH and VV polarizations) as a function of depression angle (21 July 1965)

Figures 13 through 15 illustrate directly the wind dependence of the differential doppler for different radar frequencies.

A summary of the results obtained with the 4FR phase data indicates:

1. The width of the spectra of radar sea-echo is frequency dependent, and decreases with increasing radar frequency.

2. The bandwidth is widest for horizontal polarization, narrowest for vertical polarization, and intermediate for the depolarized spectra.

3. The bandwidth of the spectra for all the polarizations increases with wave height.

4. The bandwidth for vertical polarization is almost independent of depression angle between 5 and 30 degrees; the bandwidth of the spectra for horizontal polarization decreases toward the width of the vertical spectra with increasing depression angle.

5. Doppler is both polarization and frequency dependent, greatest for the C and X bands and decreasing toward the P-band.

6. The differential doppler is wind dependent for small and intermediate winds (0 to 30 knots) and seems to saturate at higher winds (above 40 knots).

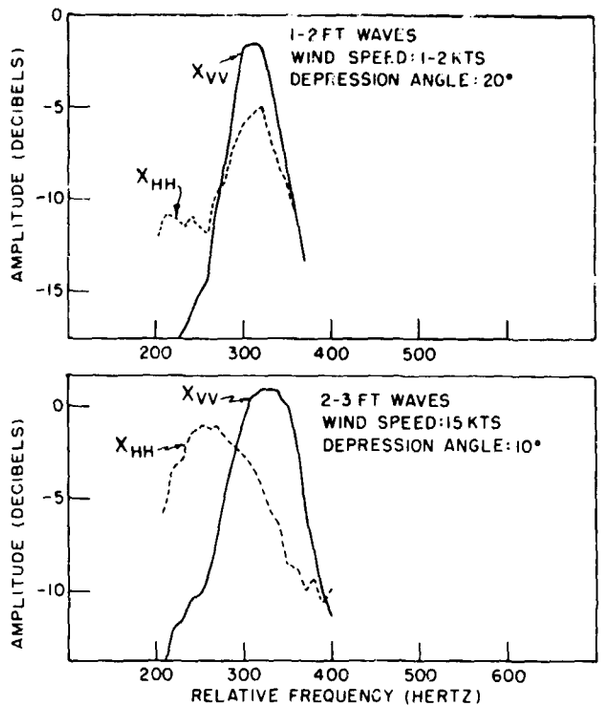

Fig. 13 - Wind dependence of the differential doppler of spectra of radar sea-echo (X-band, 29 July 1965)

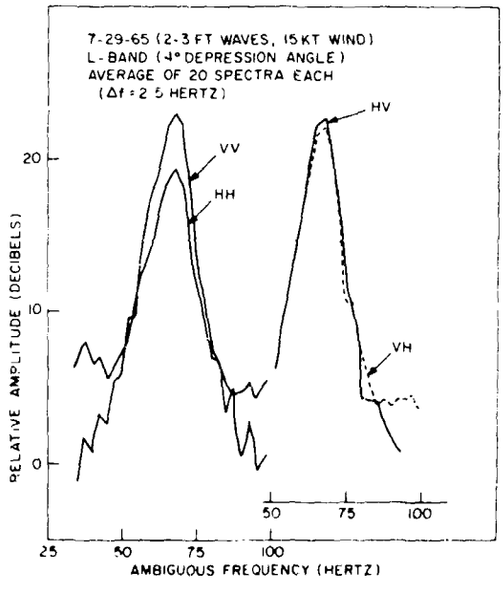

Fig. 14 - Doppler spectra of radar sea-echo for L-band, all polarizations (29 July 1965)

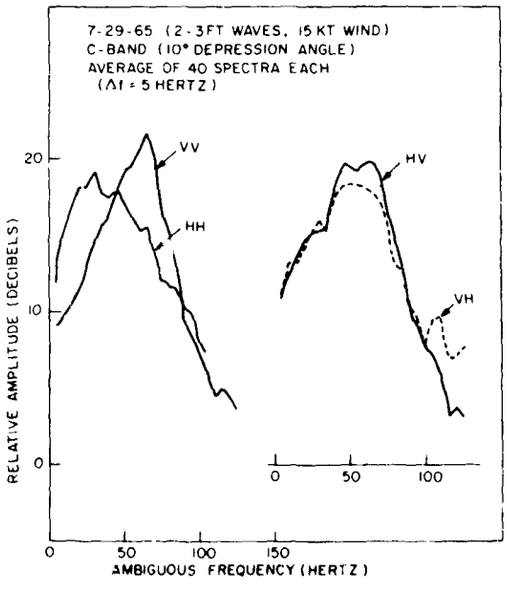

Fig. 15 - Doppler spectra of radar sea-echo for C-band, all polarizations (29 July 1965)

7. The bandwidth of the spectra seems to be greatest upwind, intermediate for crosswind, and smallest for downwind.

Work will continue in the development of a more realistic electromagnetic scattering model in which an air plus wind-blown spray and water boundary is used. In order to achieve this, it would be very desirable to have more quantitative results on spray over the sea.

ACKNOWLEDGMENTS

The authors thank Dr. J. W. Wright of the Naval Research Laboratory for the helpful exchange of ideas with him and also thank their Branch Head, Mr. N. W. Guinard, for his critical review of the manuscript.

REFERENCES

1. Rice, S.O., "Reflection of Electromagnetic Waves from Slightly Rough Surfaces," Comm. Pure Appl. Math. 4:351-378 (1951)

2. Peake, W.H., "Theory of Radar Return from Terrain," IRE National Convention Record, Vol. 7, Part I, pp. 27-41, 1959

3. Valenzuela, G.R., "Depolarization of EM Waves by Slightly Rough Surfaces," IEEE Trans. AP-15:552-557 (July 1967)

4. Wright, J.W., "A New Model for Sea Clutter," IEEE Trans. AP-16:217-223 (Mar. 1968)

5. Valenzuela, G.R., "Scattering of Electromagnetic Waves from a Tilted Slightly Rough Surface," Radio Science 3:1057-1066 (Nov. 1968)

6. Crombie, D.D., "Doppler Spectrum of Sea Echo at 13.56 Mc./s.," Nature 175:681-682 (Apr. 1955)

7. Wright, J.W., "Backscattering from Capillary Waves with Application to Sea Clutter," IEEE Trans. AP-14:749-754 (Nov. 1966)

8. Ament, W.S., Burkett, J.A., Macdonald, F.C. and Ringwalt, D.L., "Characteristics of Radar Sea Clutter: Observation at 220 Mc," NRL Report 5218, Nov. 19, 1958

9. Hicks, B.L., Knable, N., Kovaly, J.J., Newell, G.S., Ruina, J.P. and Sherwin, C.W., "The Spectrum of X-Band Radiation Backscattered from the Sea Surface," J. Geophys. Res. 65:825-837 (1960)

10. Pidgeon, V.W., "Doppler Dependence of Radar Sea Return," J. Geophys. Res. 73: 1333-1341 (1968)

11. Phillips, O.M., "The Dynamics of the Upper Ocean," London:Cambridge University Press, 1966, p. 22 ff

12. Kinsman, B., "Wind Waves," Englewood Cliffs, N.J.:Prentice Hall, 1965, pp. 248-258

13. Kinsman, B., "Wind Waves," Englewood Cliffs, N.J.:Prentice Hall, 1965, pp. 241-282

14. Longuet-Higgins, M.S., "The Statistical Analysis of a Random, Moving Surface," Phil. Trans. A249:321-387 (1957)

15. Bye, J.A.T., "The Wave-Drift Current," J. Marine Res. 25:95-102 (1967)

16. Phillips, O.M., "The Dynamics of the Upper Ocean," London:Cambridge University Press, 1966, p. 109 ff

17. Kinsman, B., "Wind Waves," Englewood Cliffs, N.J.:Prentice-Hall, 1965, pp. 386-403

18. Guinard, N.W., Ransone, J.T., Jr., Laing, M.B. and Hearton, L.E., "NRL Terrain Clutter Study, Phase I," NRL Report 6487, May 10, 1967

19. Ridenour, L.N., ed., "Radar System Engineering," New York, McGraw-Hill, 1947, p. 658

20. Barrick, D.E., "Radar Signal Distortions Produced by Volume and Surface Distributed Scatterers," presented at 1968 URSI Spring Meeting, Washington, D.C.

Appendix A

PARAMETERS OF THE FOUR-FREQUENCY RADAR SYSTEM

Table A1

Radar Frequency (MHz)	Long-Term Frequency Stability (maximum parts/day)	Short-Term Frequency Stability (maximum parts/0.01 sec)	Peak Power (kW)	Average Power (W)	Peak Power Special Mode (W)	Interpulse Phase Stability (maximum degrees)	Output Tube
428 (P-band)	1 in 10^6	5 in 10^9 - 10^8	35-40	140	10	4	7651 tetrode (RCA)
1228 (C-band)	1 in 10^6	5 in 10^9 - 10^8	35-40	140	10	4	7651 tetrode (RCA)
4455 (C-band)	1 in 10^6	5 in 10^9 - 10^8	25	100	10	5	SAC-290 Klystron (Sperry)
8910 (X-band)	1 in 10^6	5 in 10^9 - 10^8	40	160	10	6	V24C Klystron (Varian)

Table A2
Principal Parameters of Four-Frequency Radar System —
Signal and Display Parameters

Repetition Rates	Submultiples of 81.959 kHz: 100.45, 200.90, 301.35, 394.07, 512.30, 602.71, 683.07, 788.16, 1463, 2926 Hz
Pulse Widths	0.1, 0.25, 0.5, 1, 2 μsec
Noise Figure	9-11 including all rf losses
IF Amplifier	
Center Frequency	37 MHz
Bandwidth	10, 4, 2, 1, 0.5 MHz
Type	lin-log, 25 and 50 dB dynamic range Limiting
Quantity	Two — One for horizontally polarized signals — One for vertically polarized signals
Range Gate	
Width	0.1, 0.2, 0.5, 1, 3, 5 μsec
Increment Readout	1 yard
Range Marks	
Width	1.0, 2.0, 5.0, 20 μsec
Spacing	1, 5, 20 nautical miles
Video System	
Consoles	Total 3: 2 operators and 1 master control
Displays	Dual-beam A scope, B scope and PPI for each console. All flat face tubes.
CRT Size	5 inches
Signal Outputs (ungated and gated)	Vertical polarization signal amplitude Horizontal polarization signal amplitude Vertical/horizontal polarization phase Horizontal polarization/transmitted signal phase Vertical polarization/transmitted signal phase
Maximum Video Amplitude	2 volts, peak-positive

Table A3
Antenna System Performance

Radar Frequency Band	Polarization	Bandwidth (MHz)	Beamwidth (degrees)		Minor Lobe (dB)		Cross Polarization (dB)	Transmission Line Loss (dB)	Antenna Gain (dB)	Voltage Standing Wave Ratio	High Power Check
			Azimuth	Elevation	Azimuth	Elevation					
P	Horizontal	±5	12.3	40	14.5	30.0	25	0.6	17.4	<1.44:1	OK
	Vertical	±5	12.1	41.0	14.5	26.0	28	0.3	17.4	<1.38:1	OK
L	Horizontal	±5	5.5	13.8	13.4	16.0	25	0.6	25.9	<1.35:1	OK
	Vertical	±5	5.5	13.0	14.0	14.0	25	0.8	26.2	<1.28:1	OK
C	Horizontal	±10	5.0	5.0	23.2	24.5	>20	2.0	31.4	<1.55	Not Measured
	Vertical	±10	5.0	5.0	23.0	24.0	>20	2.0	31.4	<1.57	Not Measured
X	Horizontal	±10	5.0	5.3	23.6	23.5	>20	0.6	31.2	<1.30:1	OK
	Vertical	±10	4.7	5.0	23.6	24.2	>20	0.6	31.2	<1.12:1	OK

Appendix B

SEA CONDITIONS AND PERTINENT INFORMATION

Table B1
Summary of Sea Conditions

Date	Measured RMS Wave Height (ft)	Visual Wave Height (ft)	Wind Speed (knots)
July 29, 1965	0.39-0.44 (APL) 0.40-0.62 (APL)	1-2 2-3	1-2 15
July 21, 1965		3-5	8-11
Dec. 9, 1964	1.022-1.077 (APL)	6-8	12-15
Feb. 20, 1969		16	29
Feb. 11, 1969		26	46-48

Table B2
Other Radar Parameters During Measurements

Run	Depression Angle (degrees)	Altitude (ft)	Antenna Azimuth (degrees)	Indicated Aircraft Speed (knots)	Aircraft Heading (degrees)
December 9, 1964 (PRF = 788 Hz, Pulse Width = 0.5 μsec, Wind Direction = 350 degrees)					
161	3	1500	0	200 Nominal	355
162	5	1500	0	200 Nominal	170
167	10	2000	0	200 Nominal	355
170	30	2000	0	200 Nominal	170
170	30	2000	0	200 Nominal	345
July 21, 1965 (PRF = 788 Hz, Pulse Width 0.25 μsec, Wind Direction = 100 degrees)					
124A	10	5590	0	200 Nominal	270
124B	20	5590	0	200 Nominal	270
124C	30	5590	0	200 Nominal	270
124D	45	5590	0	200 Nominal	270

(Table continues)

Table B2 (Continued)

Run	Depression Angle (degrees)	Altitude (ft)	Antenna Azimuth (degrees)	Indicated Aircraft Speed (knots)	Aircraft Heading (degrees)
125A	10	5590	0	200 Nominal	84
125B	20	5590	0	200 Nominal	84
125C	30	5590	0	200 Nominal	84
125D	45	5590	0	200 Nominal	84
131A	10	5590	0	200 Nominal	10
131B	20	5590	0	200 Nominal	10
131C	30	5590	0	200 Nominal	10
131D	45	5590	0	200 Nominal	10
133A	10	5590	0	200 Nominal	15
133B	20	5590	0	200 Nominal	15
133C	30	5590	0	200 Nominal	15
133D	45	5590	0	200 Nominal	15
February 11, 1959 (PRF = 683 Hz, Pulse Width = 0.5 μsec, Wind Direction = 290 degrees)					
147	5	1500	0	195	308
150	10	1500	0	195	308
151	20	1575	0	190	308
154	20	1575	180	190	308
155	10	1575	180	190	308
156	5	1575	180	190	308
157	5	1575	0	190	128
160	10	1575	0	190	138
161	20	1575	0	190	128
2	20	6750	350	192	220
3	30	6750	350	192	220
10	30	6750	170	192	220
11	20	6750	170	192	220
36	45	12,300	0	185	290
44	45	12,300	180	185	290
February 20, 1969 (PRF = 608 Hz, Pulse Width = 0.5 μsec, Wind Direction = 60 degrees)					
13	10	1500	0	200 Nominal	60
14	20	1500	0	200 Nominal	60
17	20	1500	180	200 Nominal	60
20	10	1650	180	200 Nominal	60
21	5	1650	180	200 Nominal	60
26	10	1650	0	200 Nominal	240
27	20	1650	0	200 Nominal	240
32	20	1500	180	200 Nominal	240
33	10	1500	180	200 Nominal	240

NOTE:

0° Antenna Azimuth { C and X bands, forward looking. P and L bands, backward looking.

180° Antenna Azimuth { C and X bands, backward looking. P and L bands, forward looking.

Table B3
Summary of Parameters Used to Calculate Spectra

Frequency Band	Frequency Resolution (Hz)	Number of Spectra Averaged	Length of Data for Each Spectra (sec)	Total Length of Data for Final Spectra (sec)
P	1.0	20	0.50	10
L	2.5	20	0.20	4
C	5.0	40	0.10	4
X	10.0	40	0.05	2

Table B4
Average (Over Up-Wind, Down-Wind, and Cross-Wind)
Half-Power Bandwidth of Radar Sea-Echo Spectra

Depression Angle (degrees)	Radar Frequency Band	HH (ft/sec)	VV (ft/sec)	HV or VH (ft/sec)
1/2 to 2 ft Waves, 1-2 Knot Wind				
20	L	3.48	3.11	3.39
	C	3.03	2.87	2.87
	X	2.65	1.98	2.40
30	L	3.26	2.82	3.31
	C	2.51	2.44	2.23
	X	2.27	1.99	1.88
2-3 ft Waves, 15 Knot Wind				
4	P	—	2.40	—
	L	3.82	3.82	3.67
	C	4.17	3.60	—
	X	—	2.77	2.78
10	P	3.57	4.06	2.93
	L	3.40	2.76	3.74
	C	4.10	2.65	3.43
	X	—	3.43	2.92
3-5 ft Waves, 8-11 Knot Wind				
10	P	6.61	4.77	5.28
	L	6.64	4.66	5.07
	C	5.78	4.12	5.34
	X	6.11	3.81	4.63

(Table continues)

Table B4 (Continued)

Depression Angle (degrees)	Radar Frequency Band	HH (ft/sec)	VV (ft/sec)	HV or VH (ft/sec)
20	P	5.75	5.96	6.11
	L	5.48	3.94	4.15
	C	4.92	3.98	4.00
	X	5.52	3.19	2.98
30	P	6.72	5.82	6.47
	L	4.68	4.52	5.09
	C	4.39	3.83	4.19
	X	4.76	3.85	4.06
16 ft Waves, 29 Knot Wind				
5	P	11.20	9.34	6.86
	L	10 00	7.50	8.20
	C	—	6.60	3.90
	X	7.70	6.90	8.25
10	P	8.45	10.30	9.75
	L	9.00	8.00	8.00
	C	8.80	7.45	7.70
	X	8.25	7.10	7.60
20	P	9.70	7.50	8.80
	L	7.80	6.30	6.70
	C	8.40	7.00	7.40
	X	8.00	5.60	6.23
26 ft Waves, 46-48 Knot Wind				
5	P	10.60	10.00	10.20
	L	8.00	8.50	8.95
	C	—	—	—
	X	6.00	7.40	7.11
10	P	12.40	10.60	10.45
	L	10.50	8.30	8.00
	C	—	—	10.40
	X	—	—	—
20	P	11.60	10.55	11.40
	L	11.80	9.70	10.00
	C	10.10	7.55	8.60
	X	—	7.10	8.76
30	P	13.40	10.30	11.55
	L	9.60	9.45	8.93
	C	9.10	8.55	8.55
	X	9.10	7.40	7.00

Appendix C

PARTIAL COLLECTION OF SPECTRA

The following graphs are in dB versus hertz. The labels near the top of each group are of the form:

Date

Run number	Band	Transmitter polarity	Receiver polarity

Number of averages

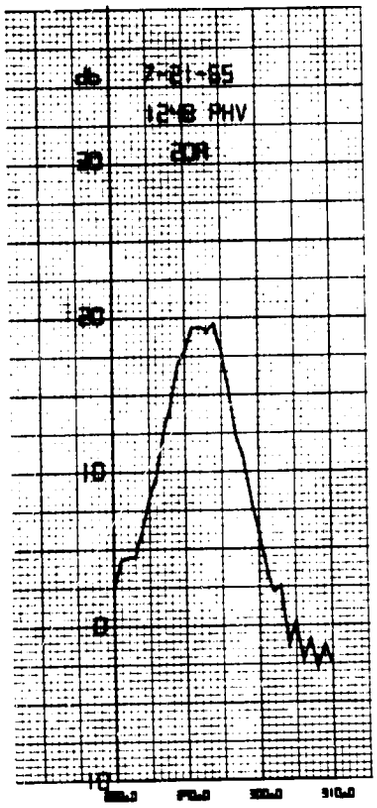
db
7-21-65
1248 PHV
20R
30
20
10
0
10

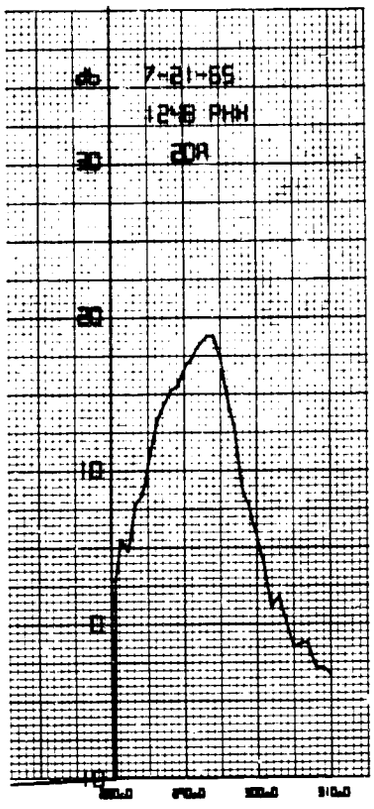
db
7-21-65
1248 PHH
20R
30
20
10
0
10

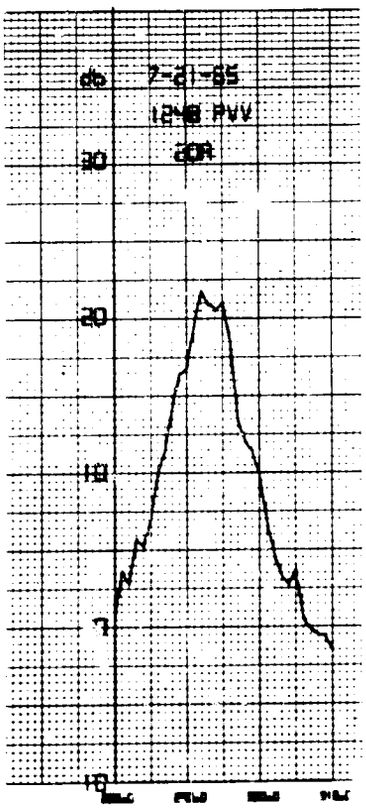
db
7-21-65
1248 PVV
20R
30
20
10
0
10

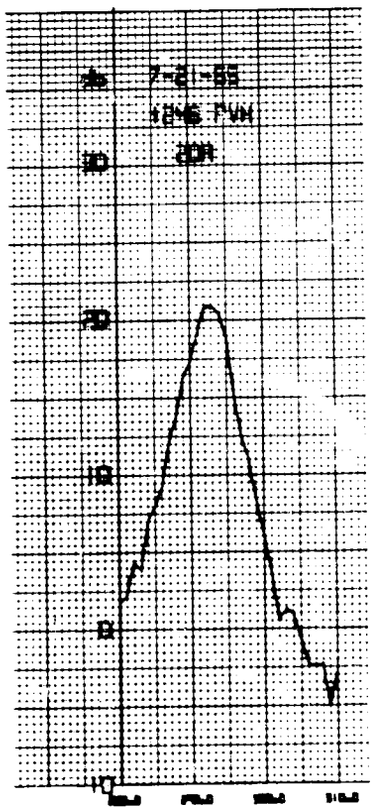
db
7-21-65
1248 PVH
20R
30
20
10
0
10

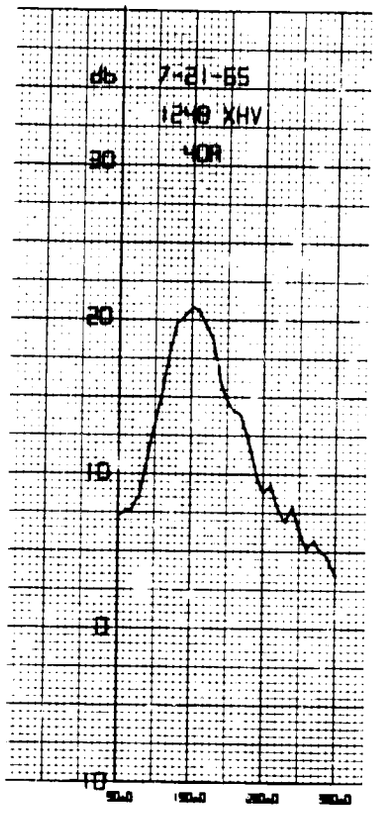
db
7-21-65
12-18 XHV
40R
30
20
10
0
10

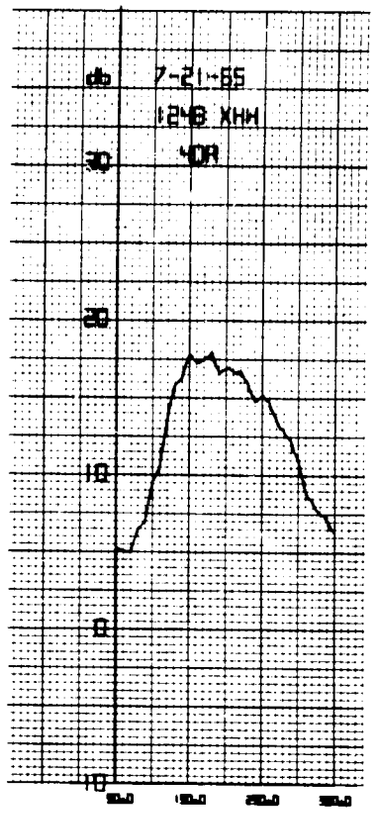
db
7-21-65
12-18 XHH
40R
30
20
10
0
10

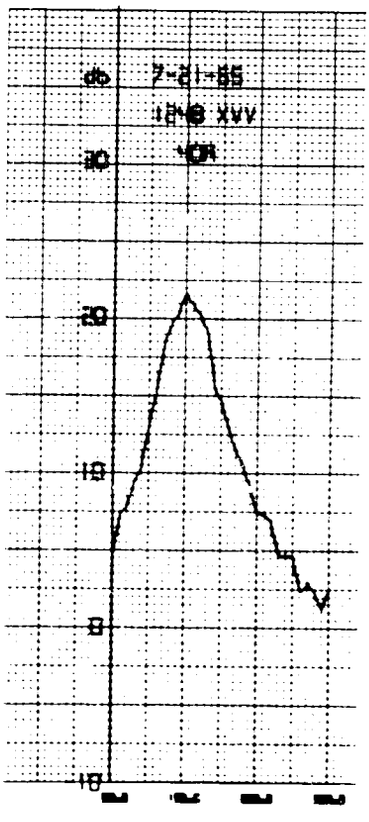
db
7-21-65
12-18 XVV
40R
30
20
10
0
10

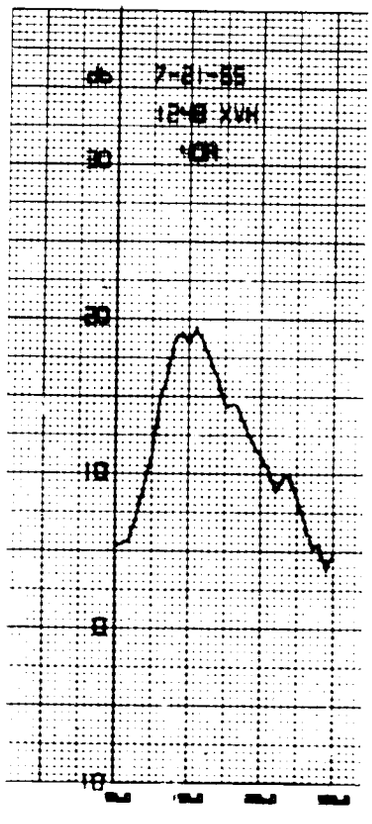
db
7-21-65
12-18 XVH
40R
30
20
10
0
10

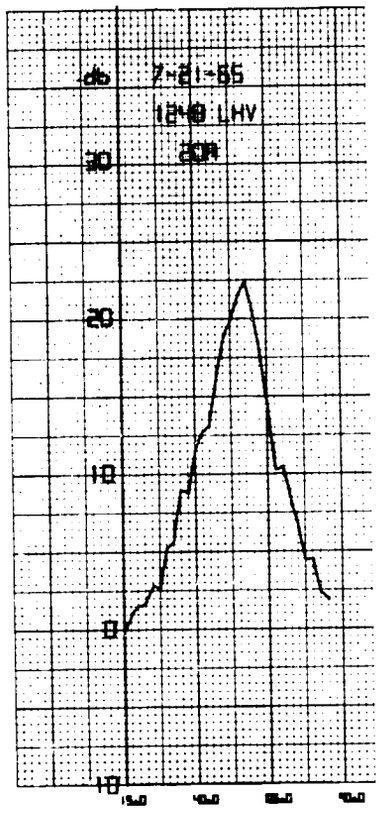
7-21-85
LHV
30
20
10
0
-10

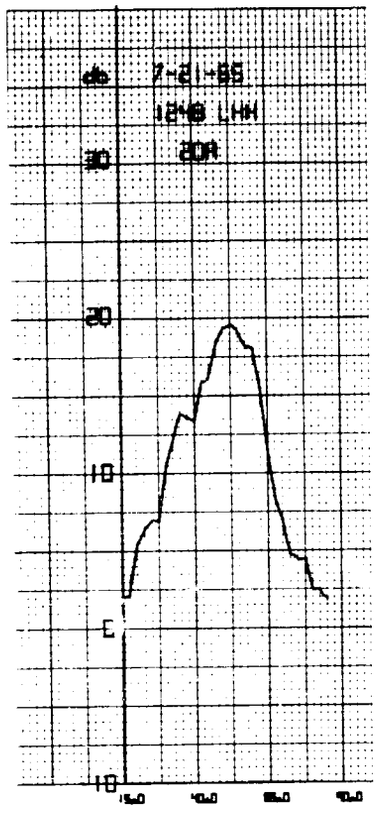
7-21-85
LHH
30
20
10
0
-10

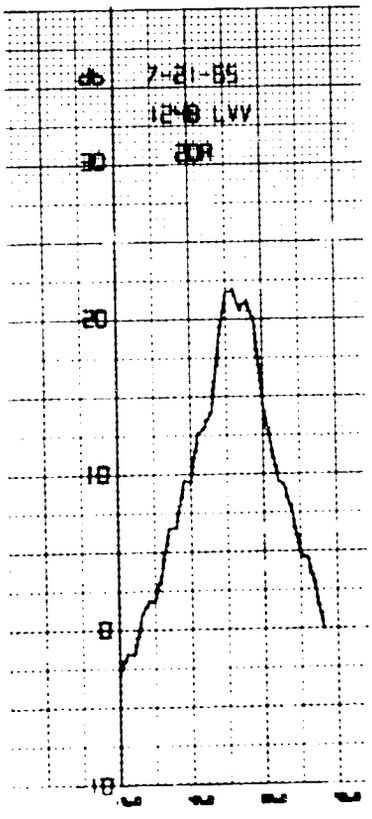
7-21-85
LVV
30
20
10
0
-10

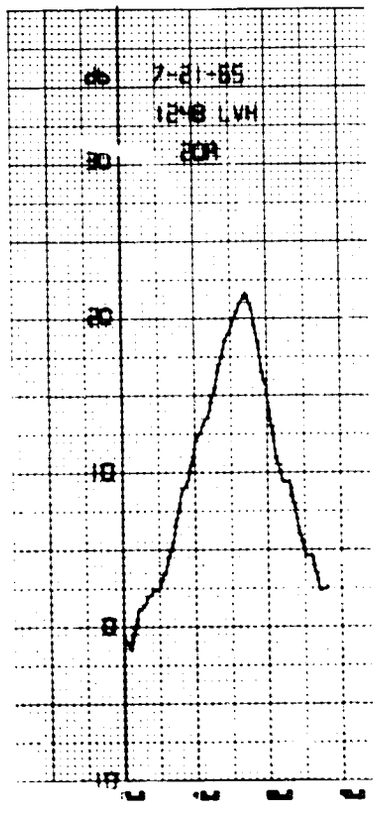
7-21-85
LVH
30
20
10
0
-10

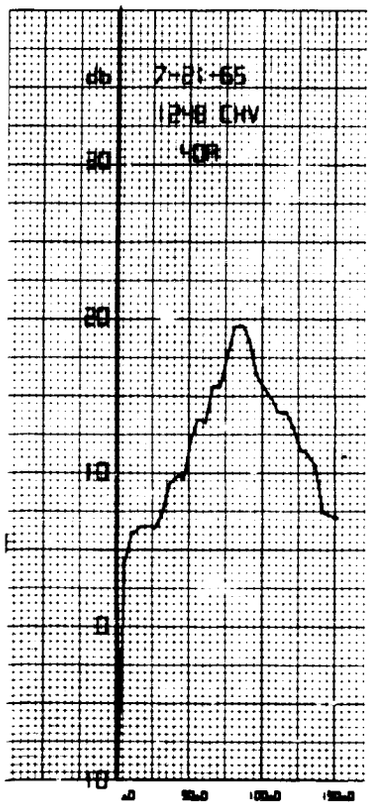
db
7-21-65
1248 CHV
40
20
10
0
-10

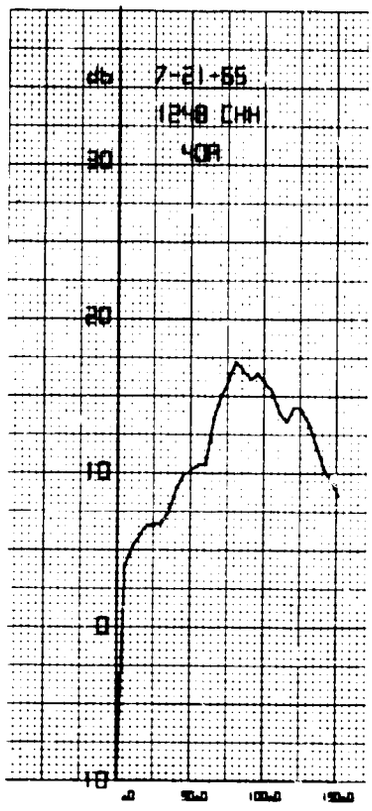
db
7-21-65
1248 CHH
40
30
20
10
0
-10

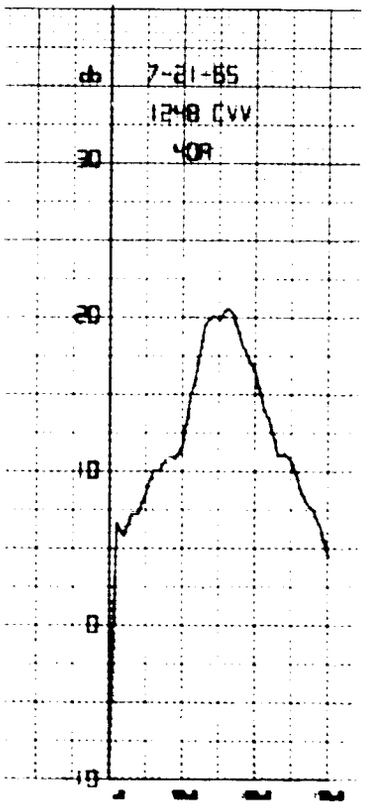
db
7-21-65
1248 CVV
40
30
20
10
0
-10

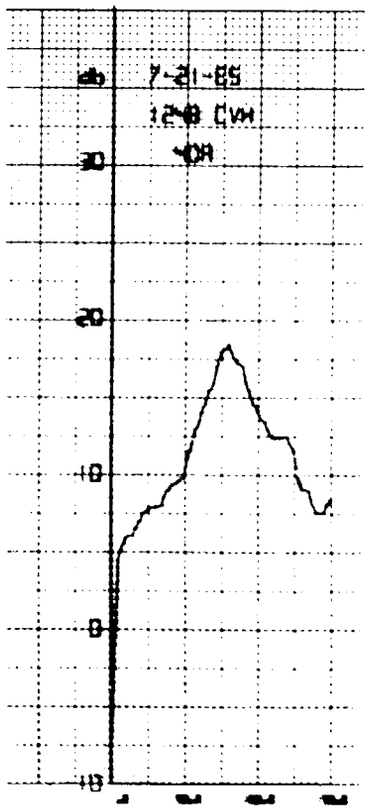
db
7-21-65
1248 CVH
40
30
20
10
0
-10

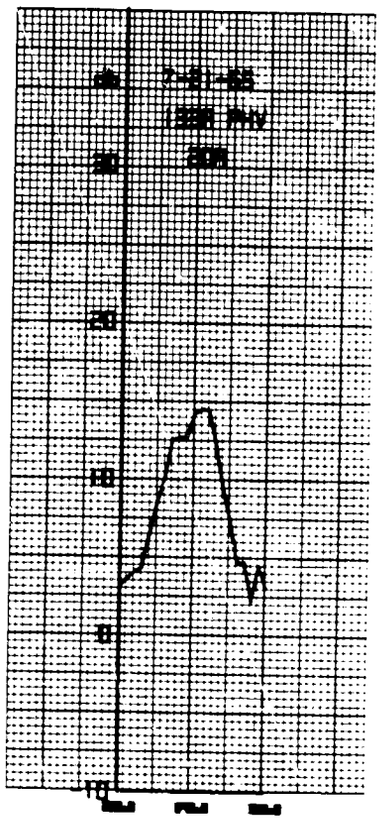

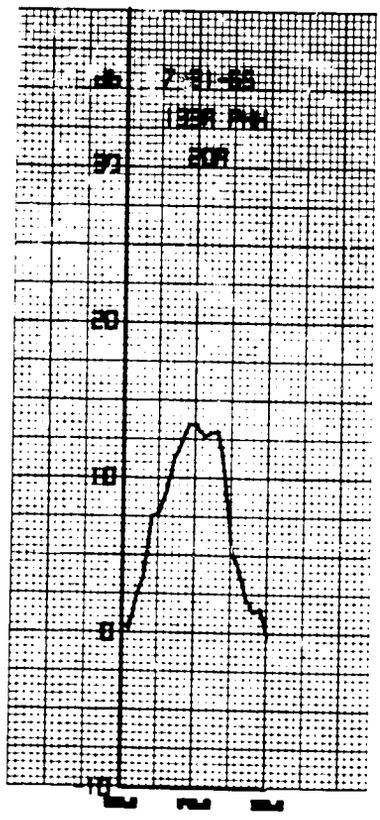

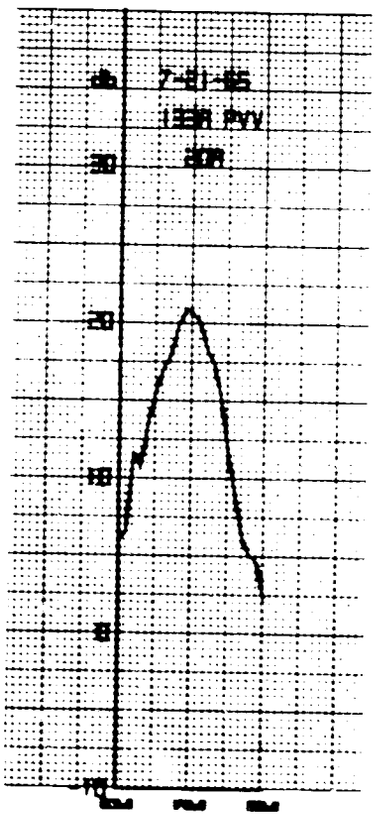

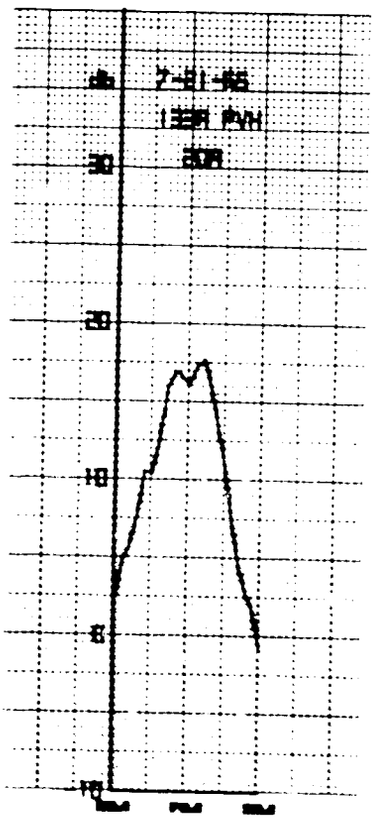

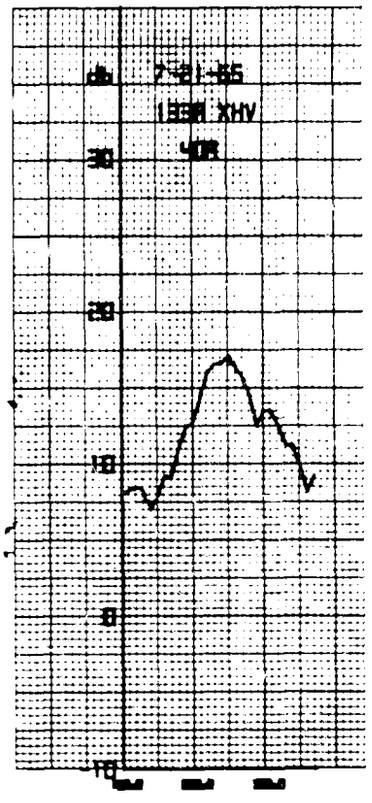
db
7-21-65
133R XHV
40R
30
20
10
0

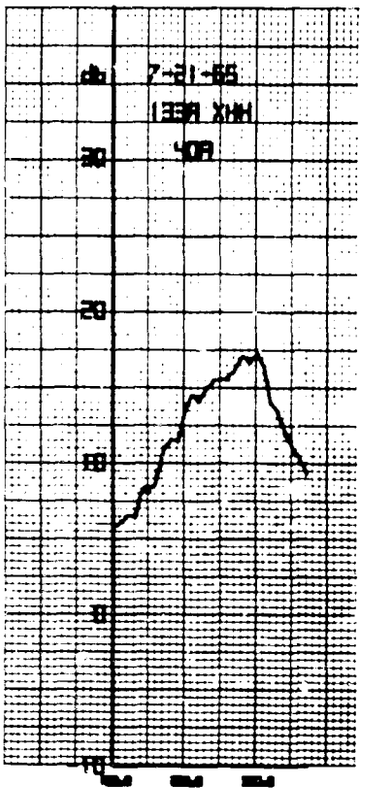
db
7-21-65
133R XHH
40R
30
20
10
0

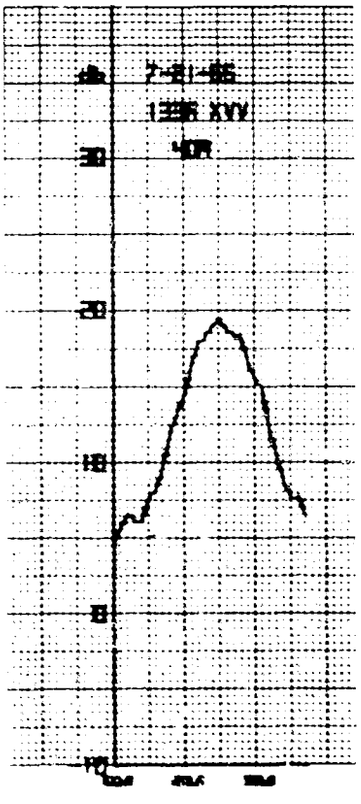
db
7-21-65
133R XVV
40R
30
20
10
0

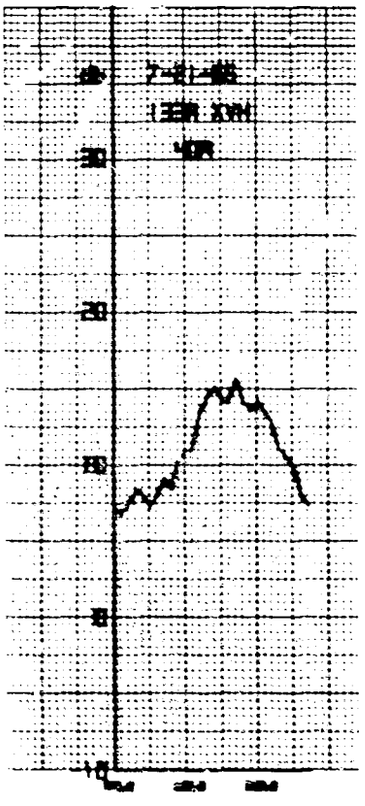
db
7-21-65
133R XHH
40R
30
20
10
0

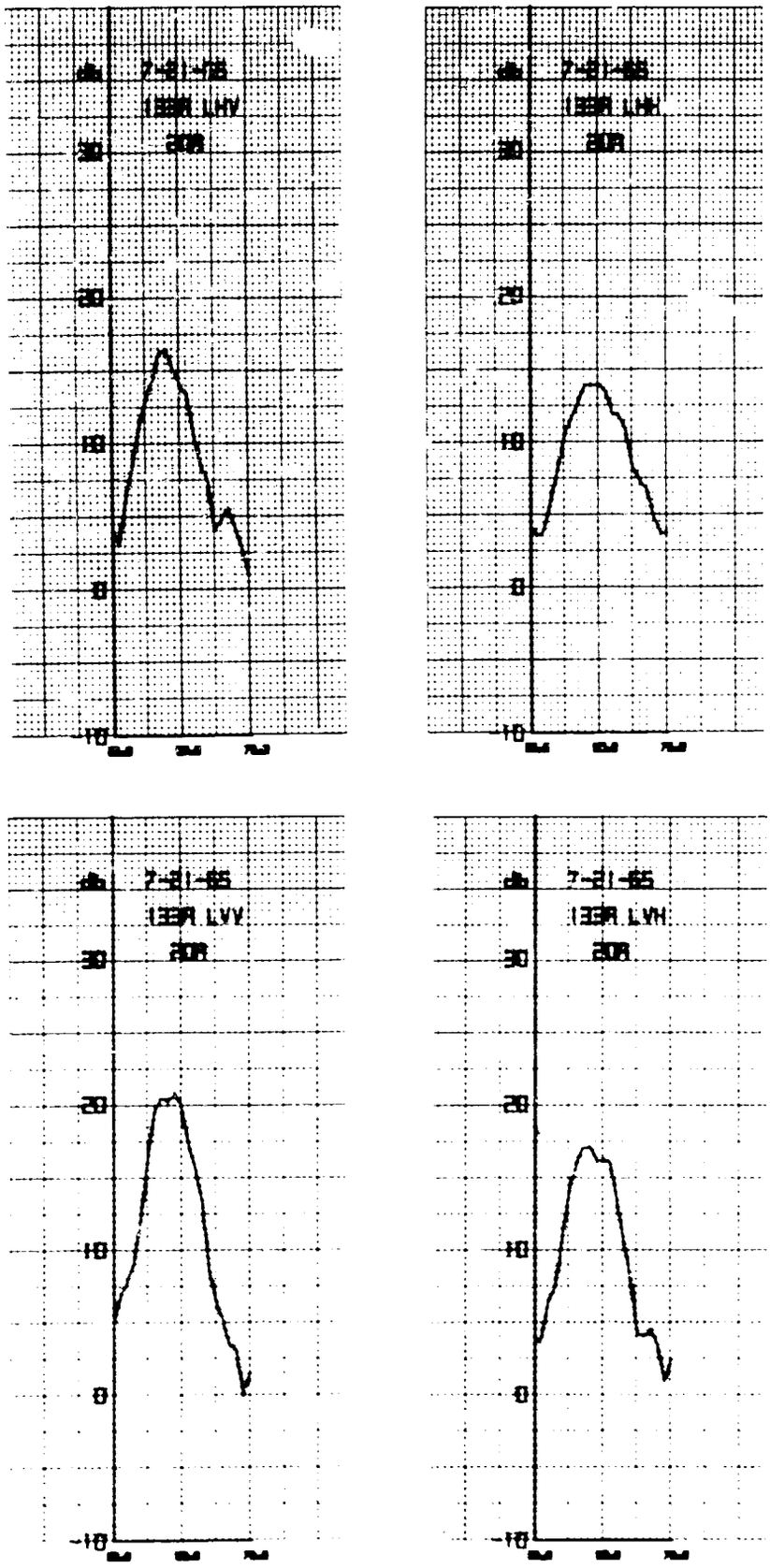
7-21-85
LHV
7-21-85
LHH
7-21-85
LVV
7-21-85
LVH

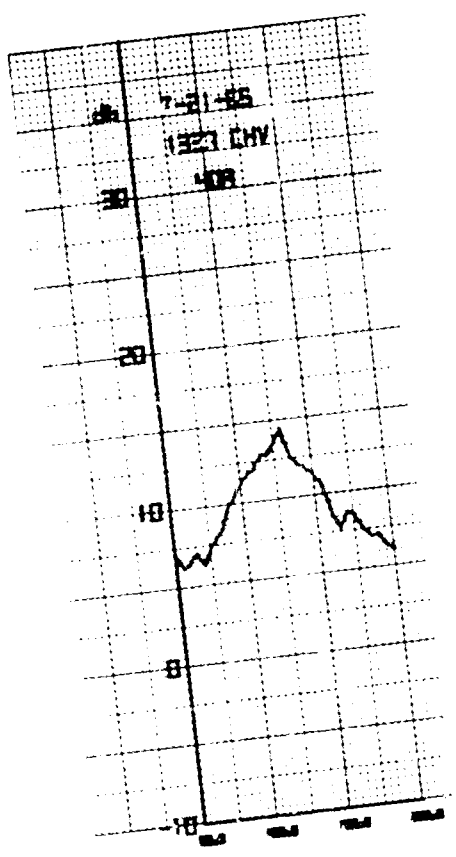
dBi
7-21-65
1323 CHV
40R
30
20
10
0
-10

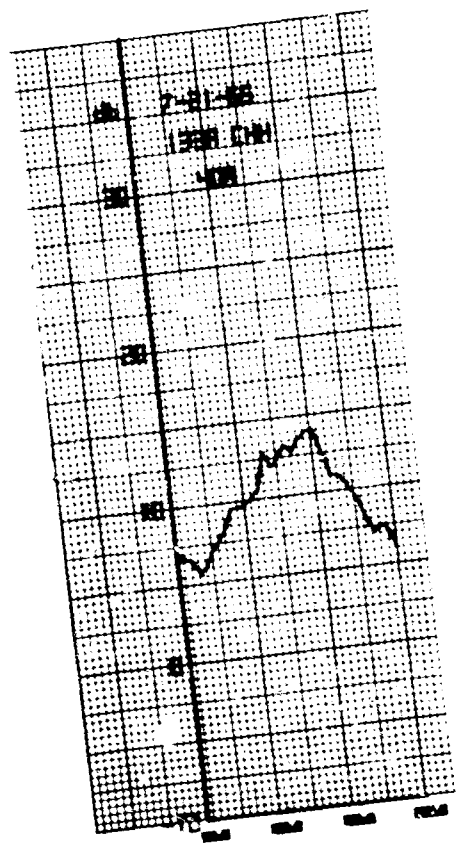
dBi
7-21-65
1388 CHH
40R
30
20
10
0
-10

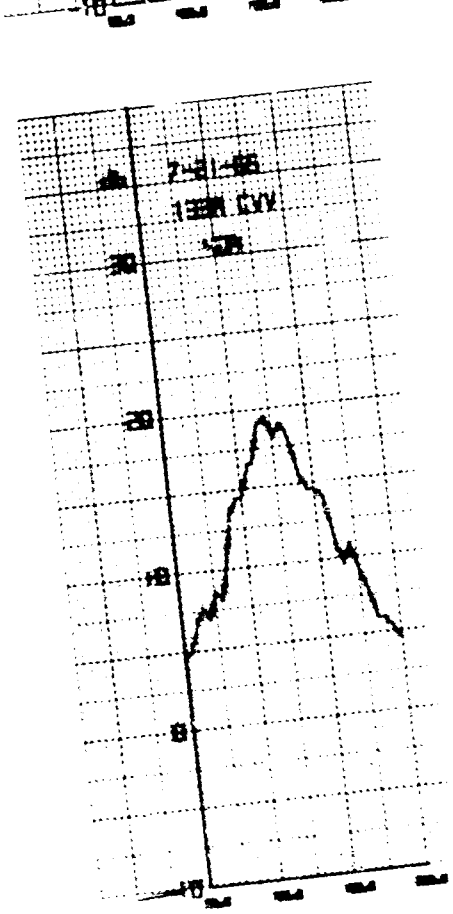
dBi
7-21-65
1338 CVV
40R
30
20
10
0
-10

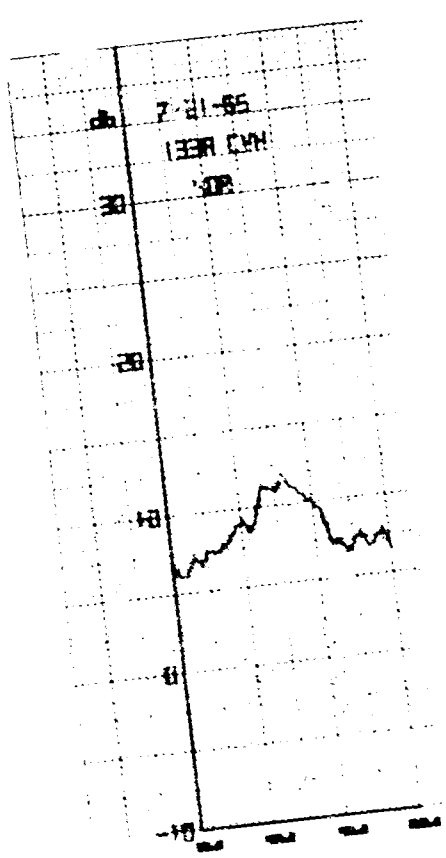
dBi
7-21-65
1338 CHH
40R
30
20
10
0
-10

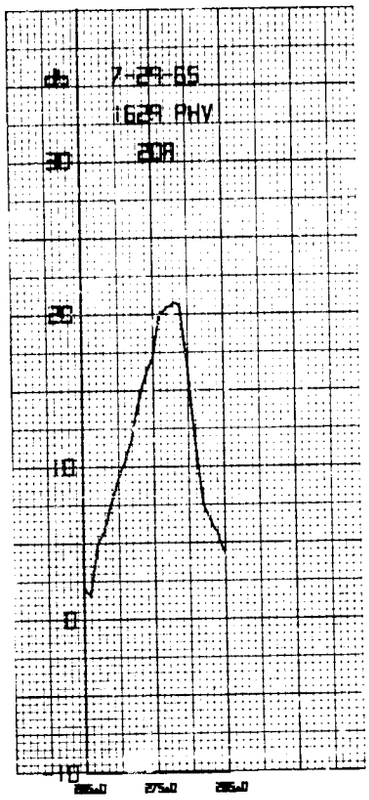
7-29-65
1628 PHV
30
20
10
0
10

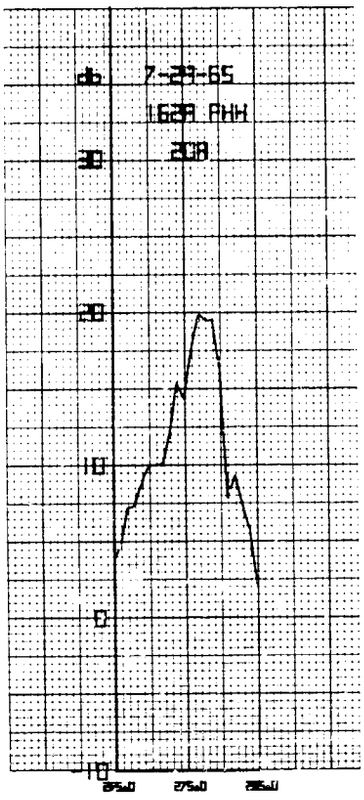
7-29-65
1628 PHH
30
20
10
0
10

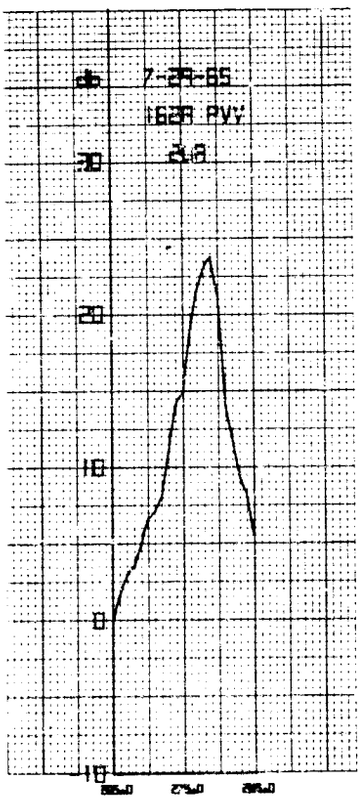
7-29-65
1628 PVV
30
20
10
0
10

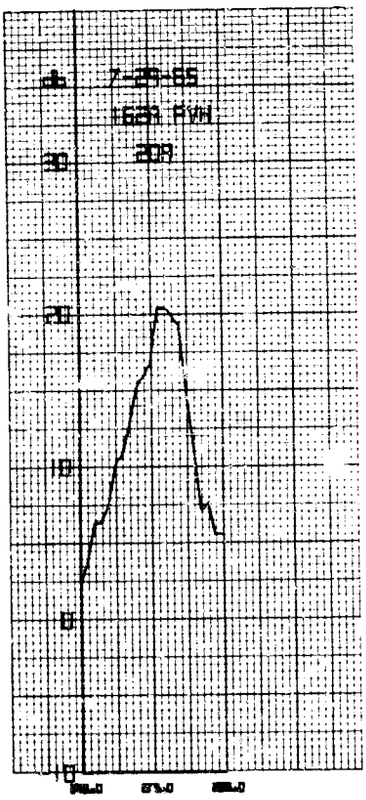
7-29-65
1628 PVH
30
20
10
0
10

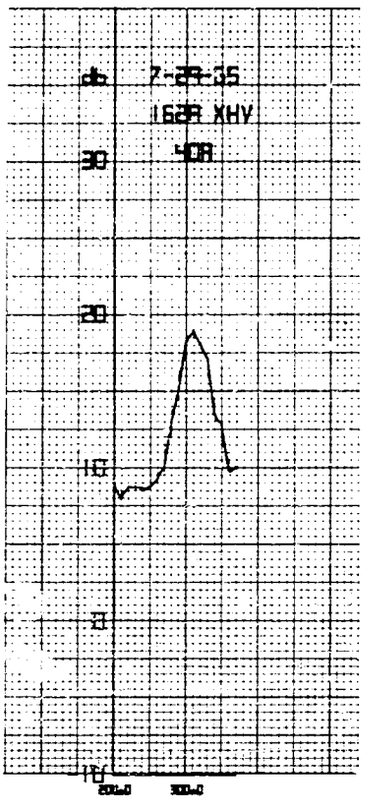

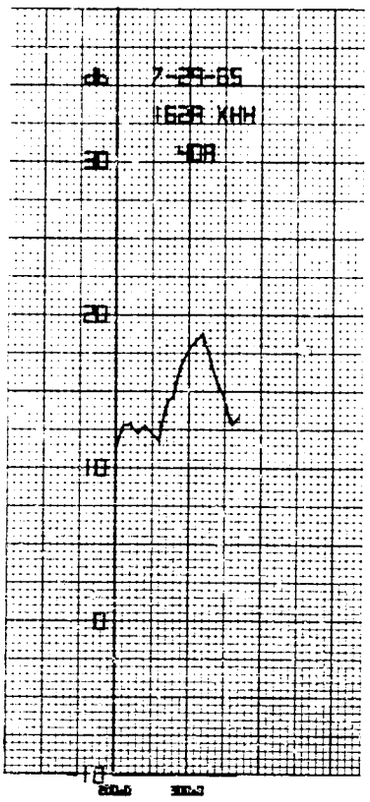

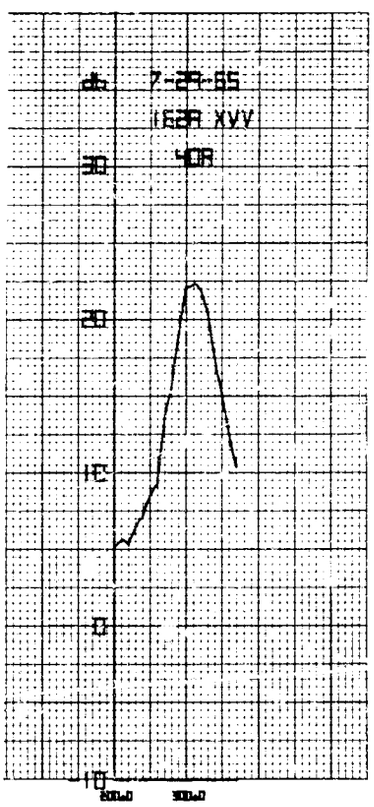

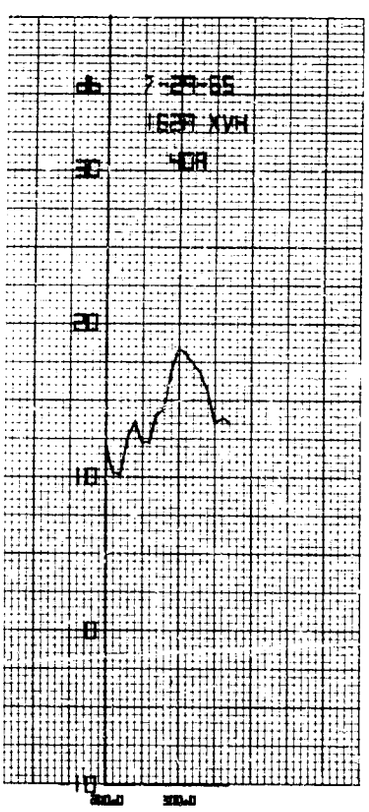

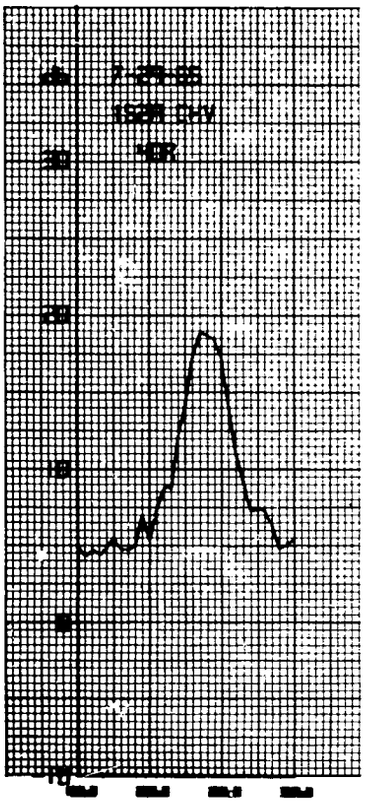

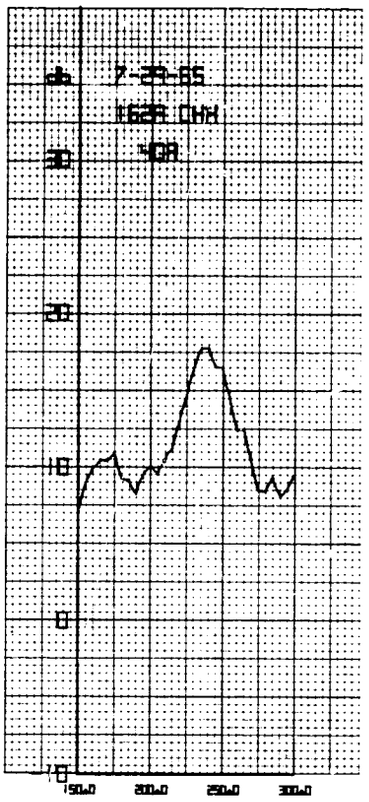

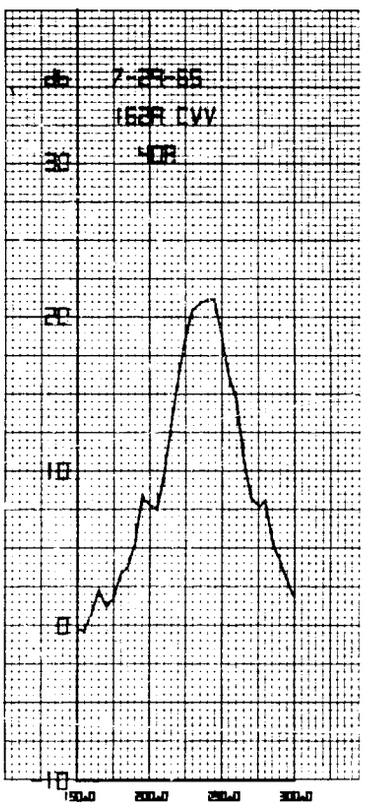

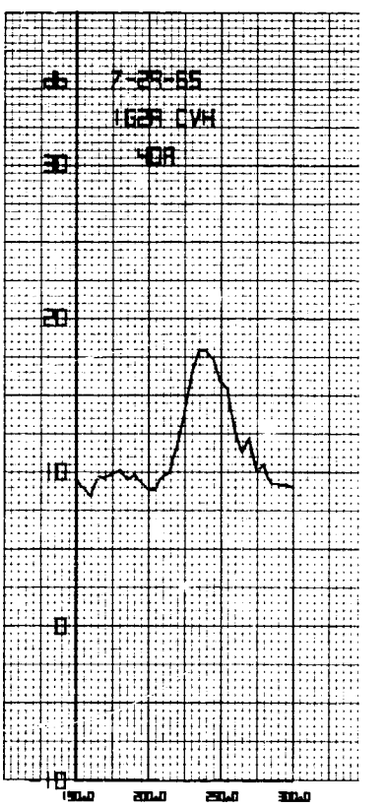

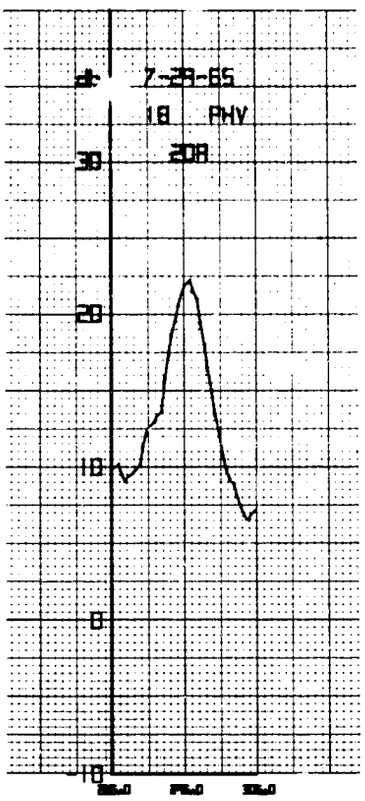
db
7-29-65
18 PHV
30 20R
20
10
0
-10

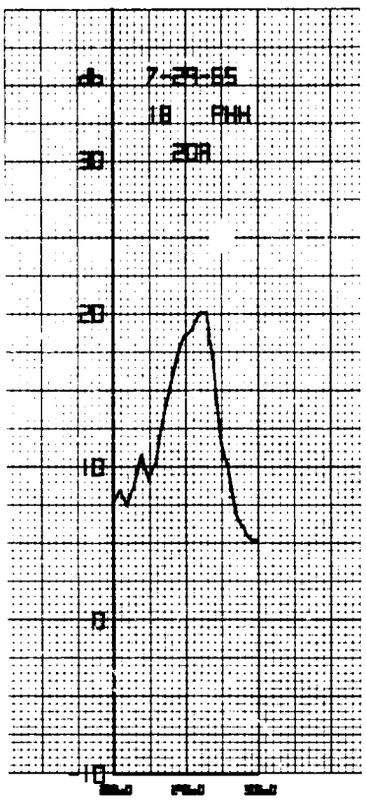
db
7-29-65
18 PHH
30 20R
20
10
0
-10

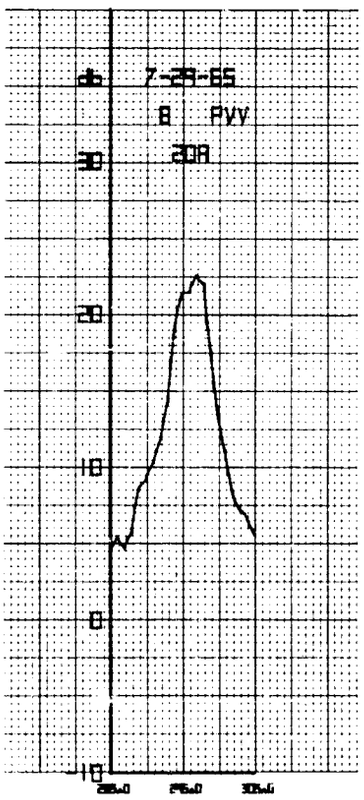
db
7-29-65
8 PVV
30 20R
20
10
0
-10

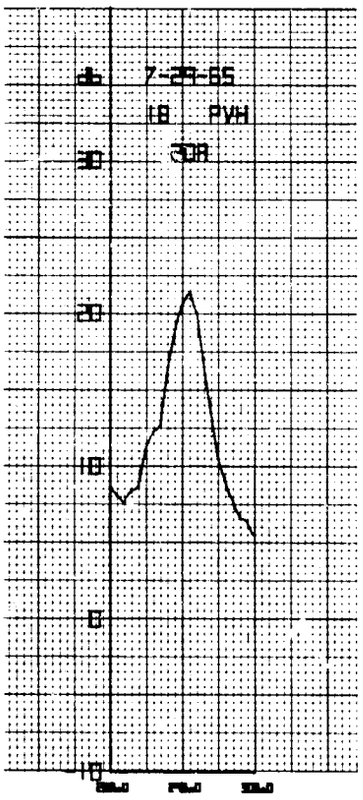
db
7-29-65
18 PVH
30 20R
20
10
0
-10

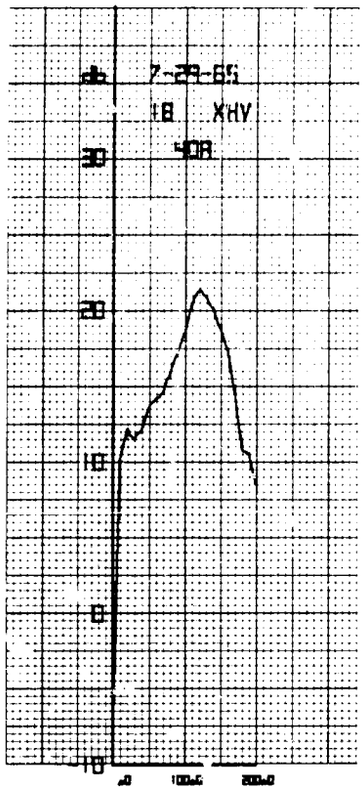
7-29-65
XHV
40
30
20
10
0
-10

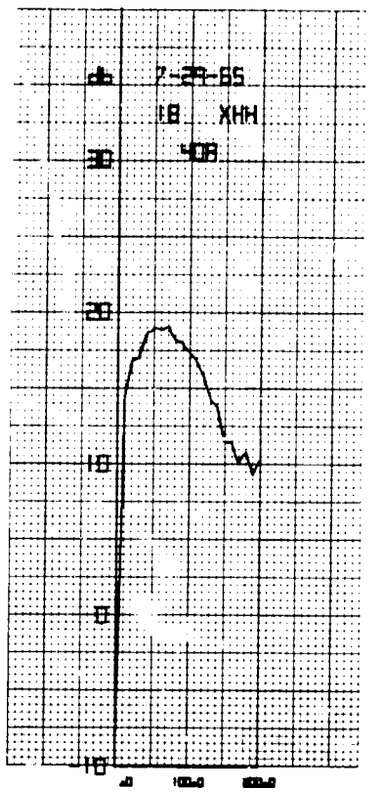
7-29-65
XHH
40
30
20
10
0
-10

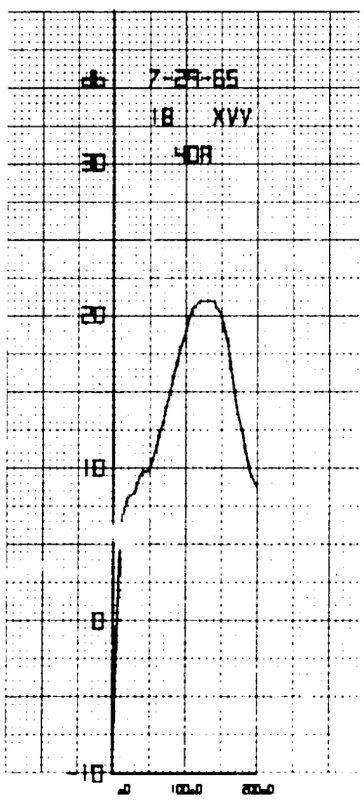
7-29-65
XVV
40
30
20
10
0
-10

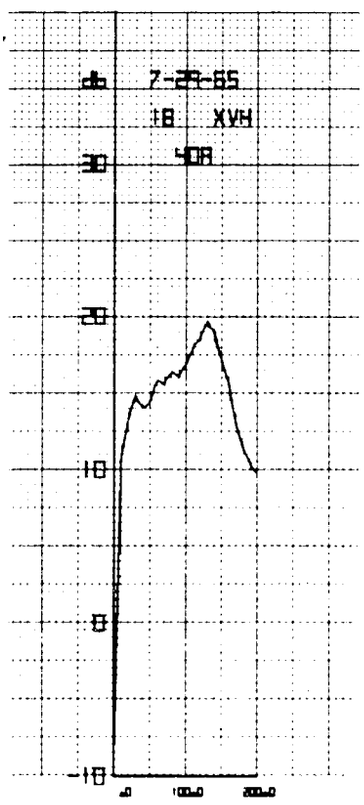
7-29-65
XVH
40
30
20
10
0
-10

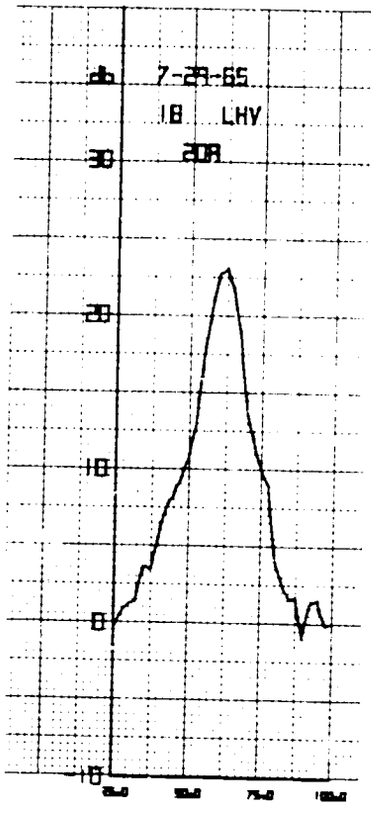
db
7-29-65
18 LHV
30 20R
20
10
0
-10

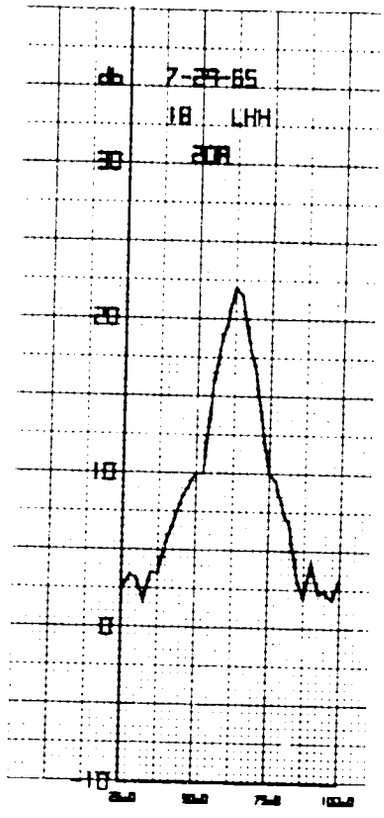
db
7-29-65
18 LHH
30 20R
20
10
0
-10

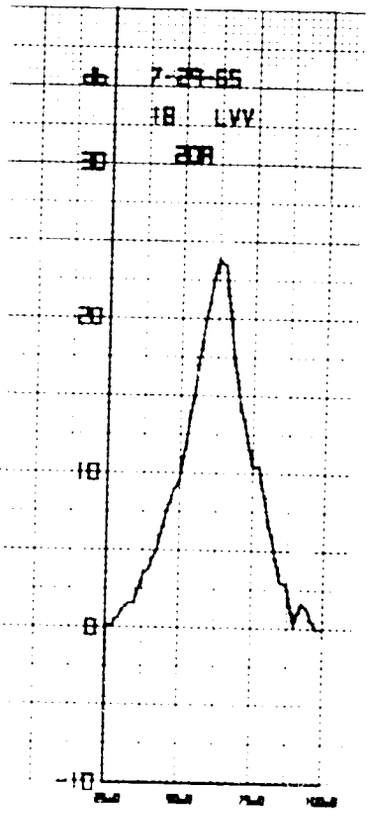
db
7-29-65
18 LVV
30 20R
20
10
0
-10

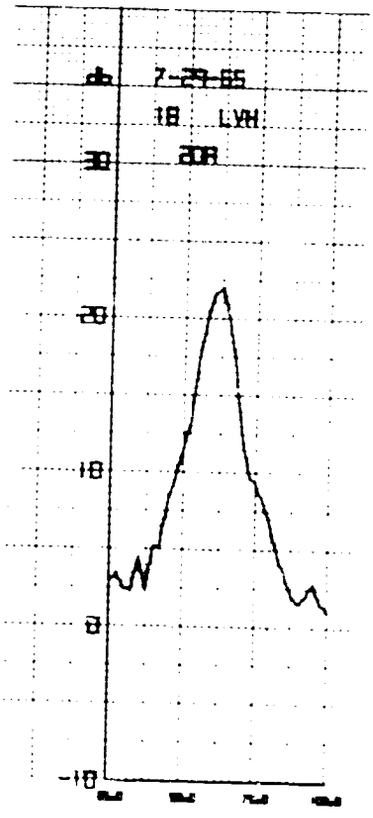
db
7-29-65
18 LVH
30 20R
20
10
0
-10

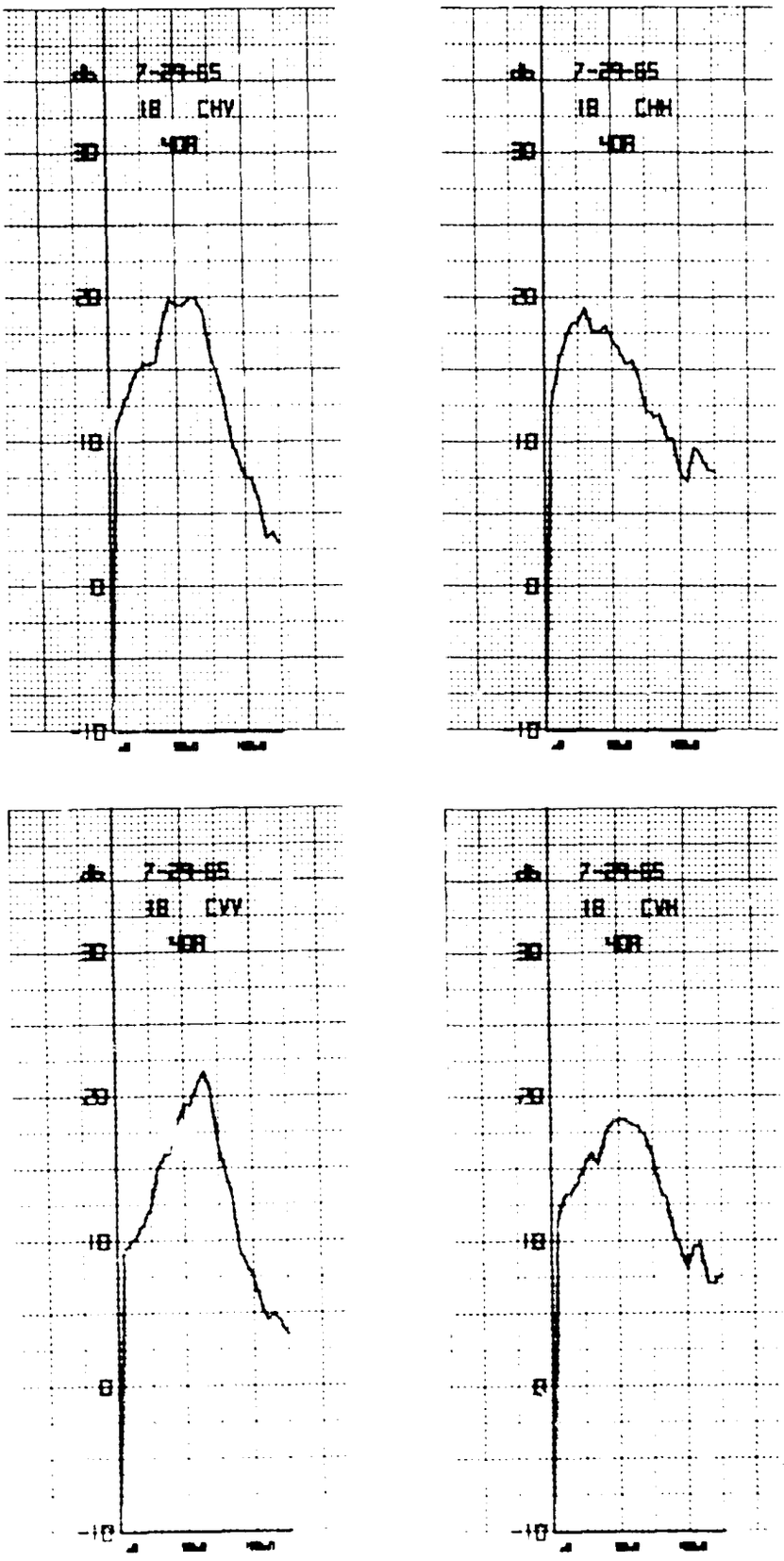
7-29-65
18 CHV
408
30
20
10
0
-10
7-29-65
18 CHH
408
30
20
10
0
-10
7-29-65
18 CVV
408
30
20
10
0
-10
7-29-65
18 CVH
408
30
20
10
0
-10

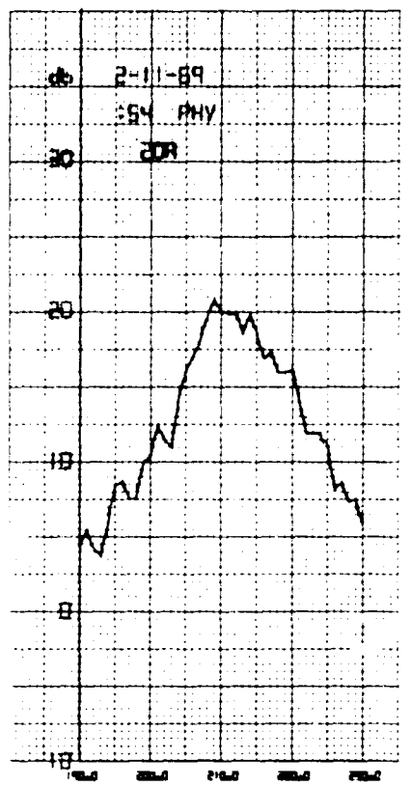

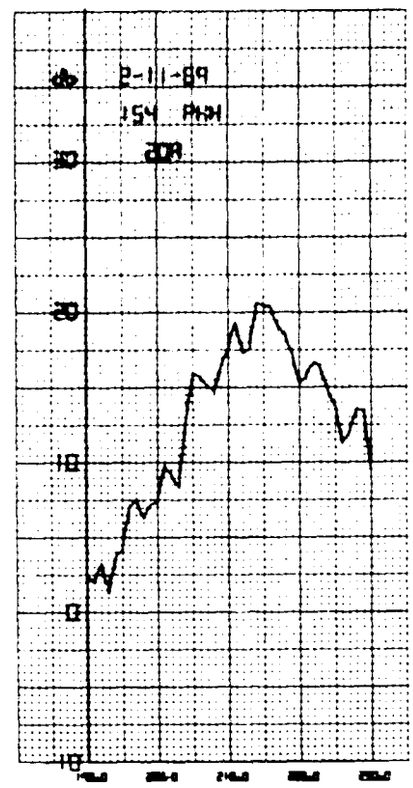

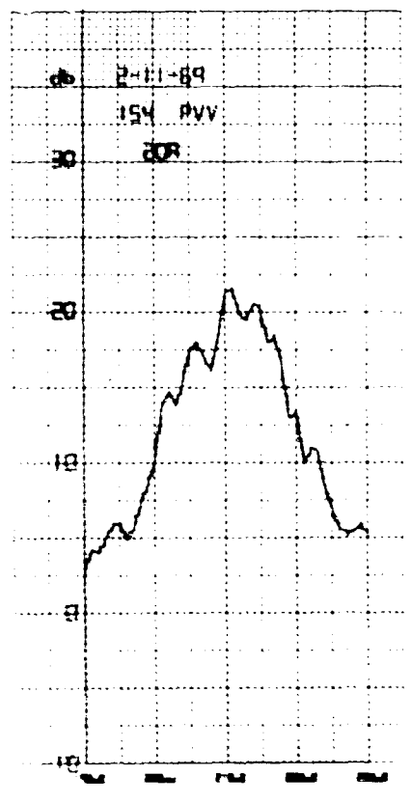

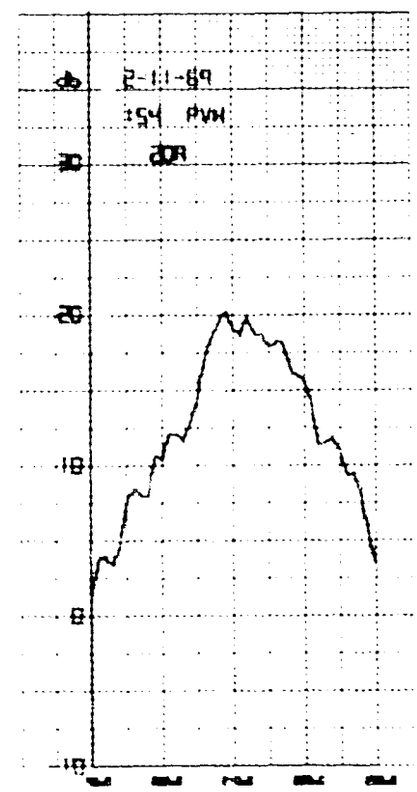

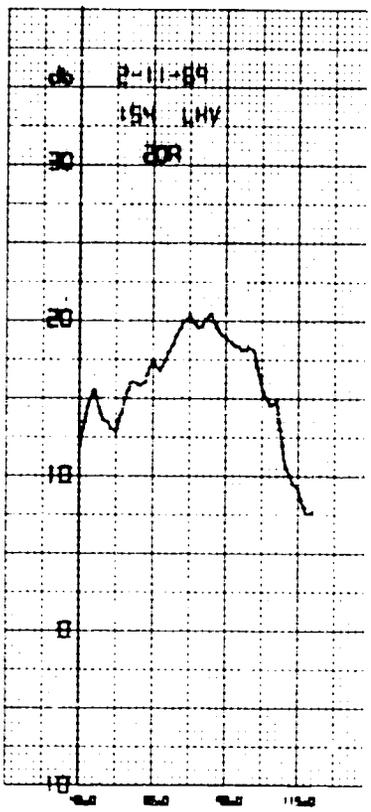

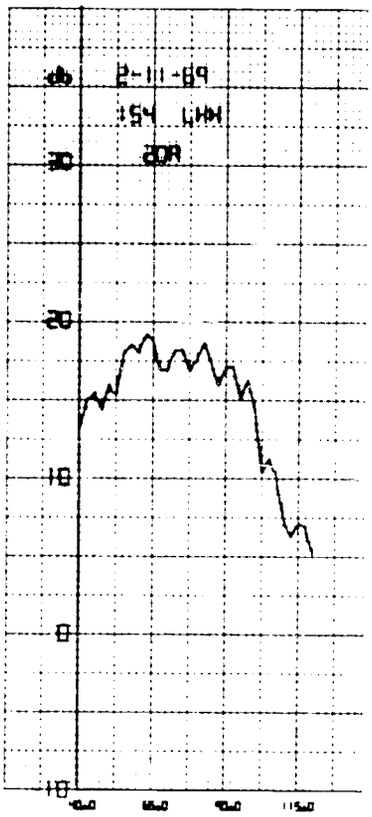

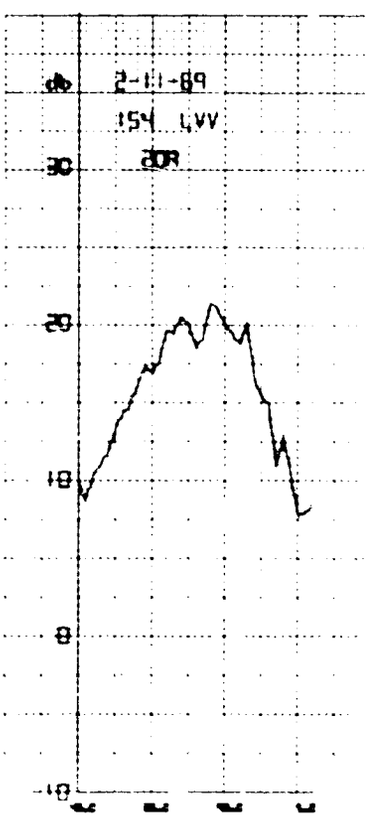

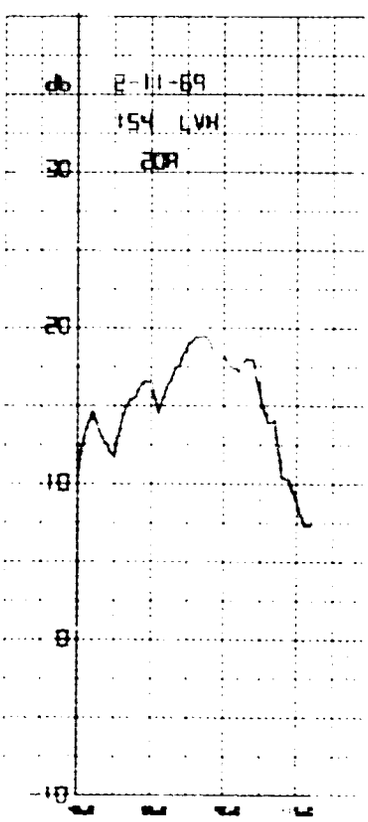

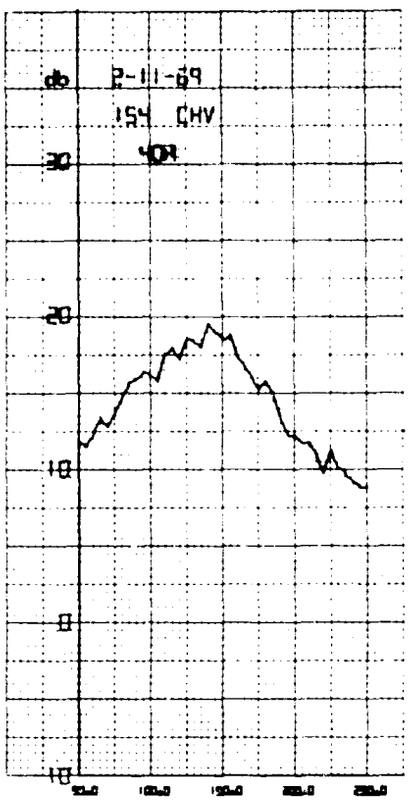

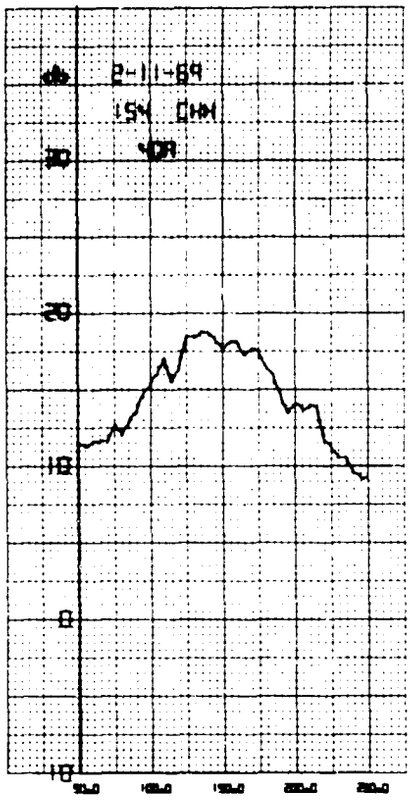

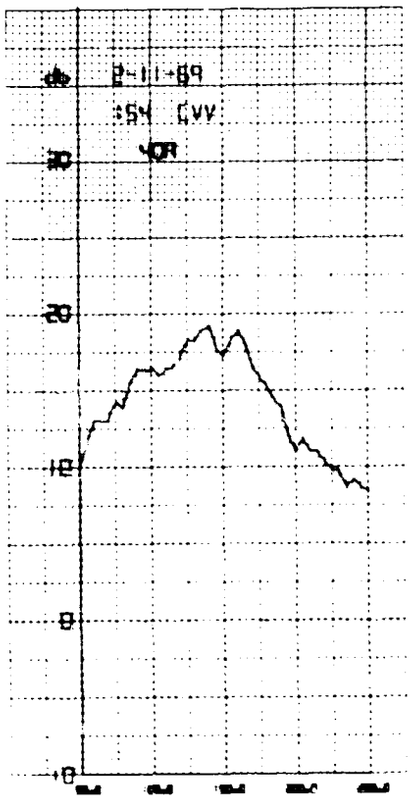

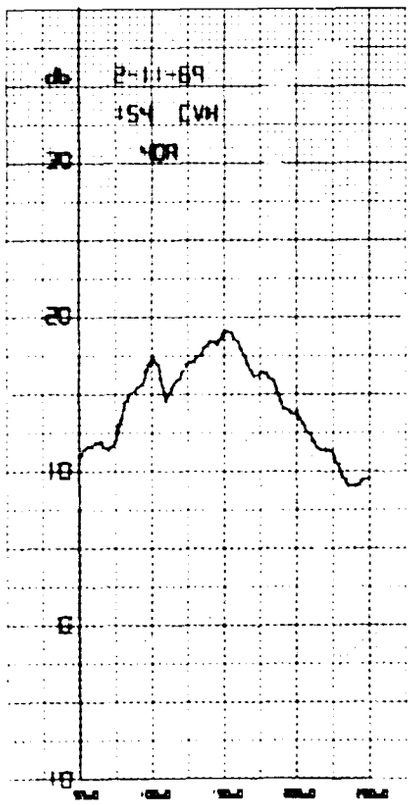

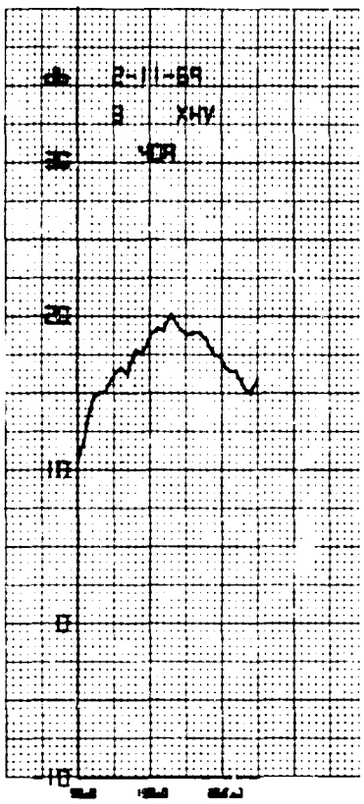

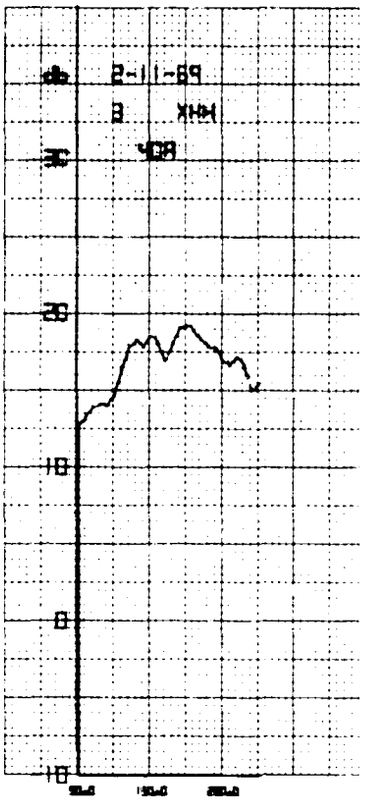

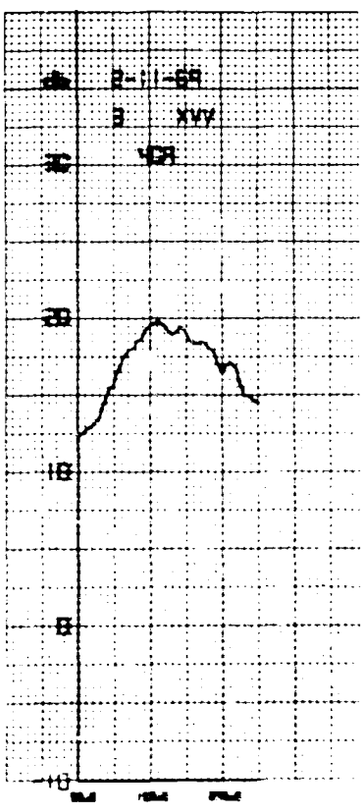

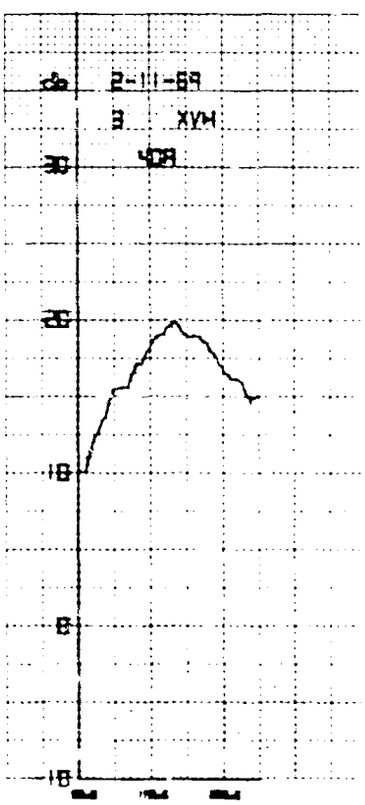

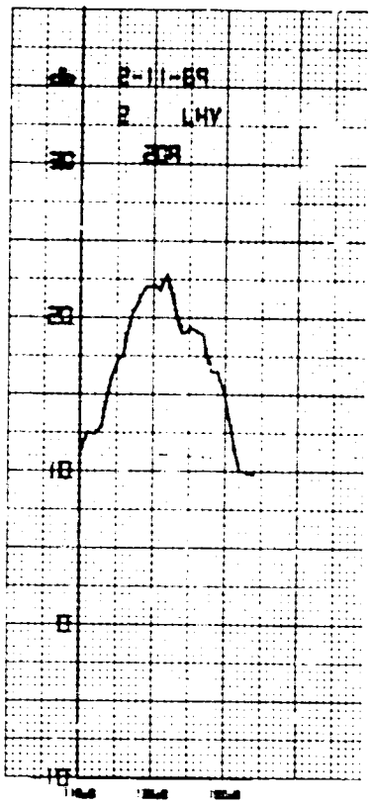
2-11-69
2 LHV

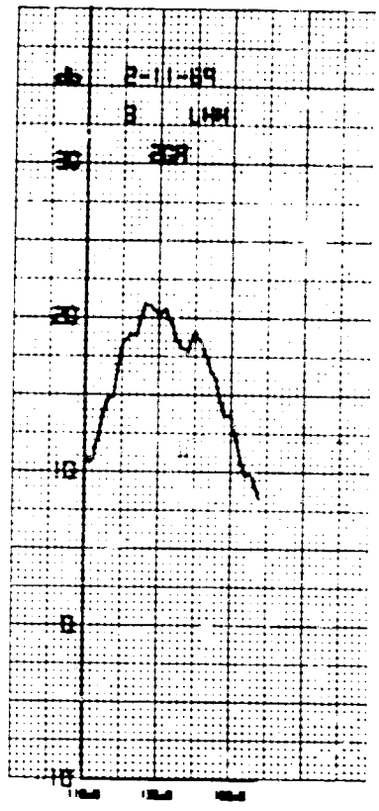
2-11-69
3 LHH

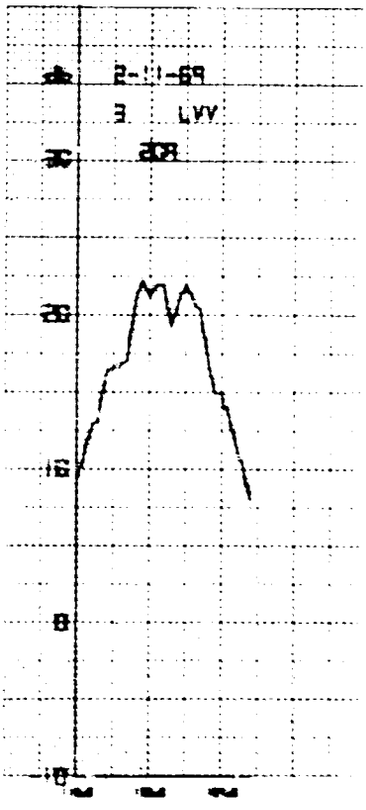
2-11-69
3 LVV

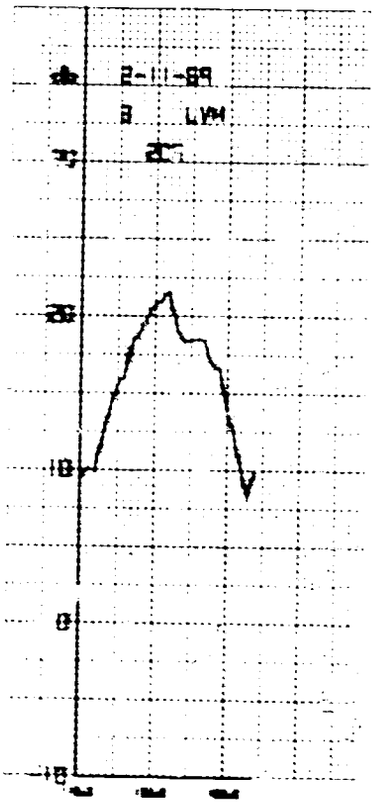
2-11-69
3 LVH

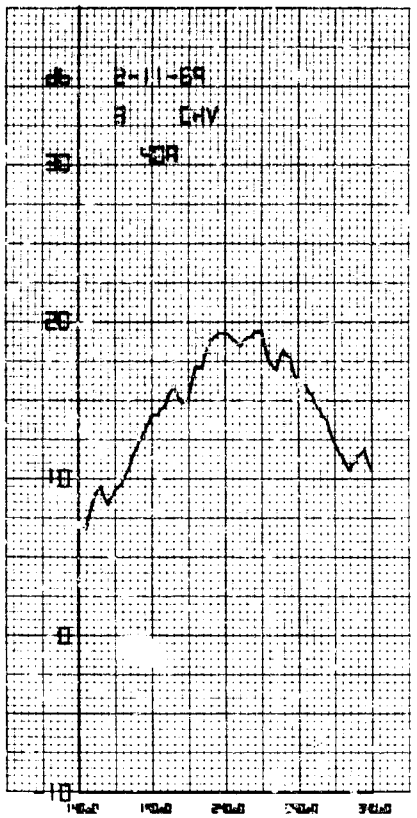

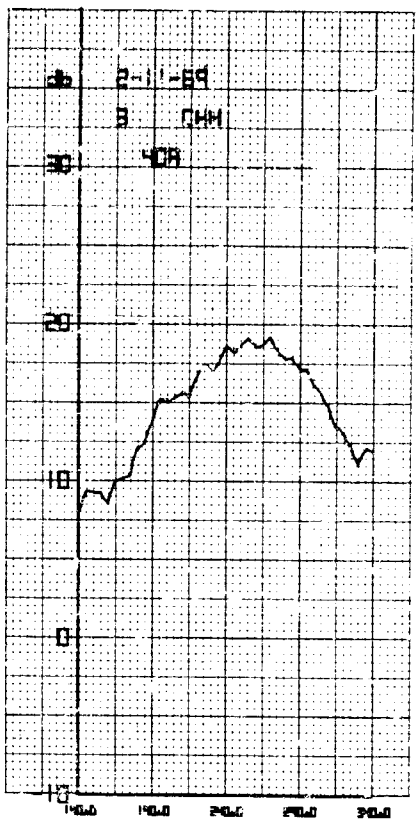

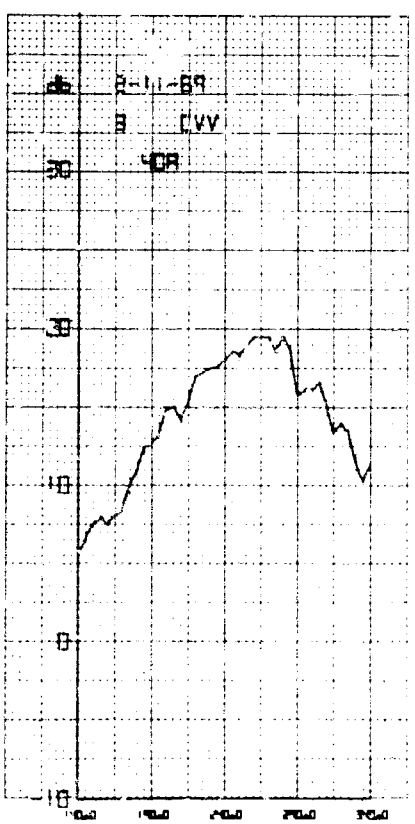

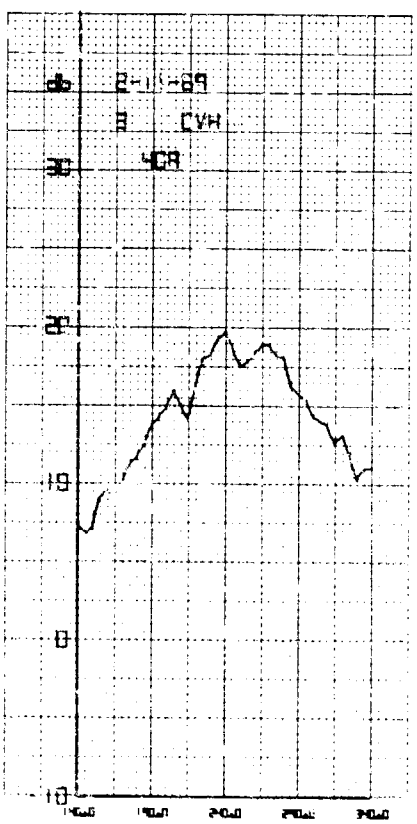

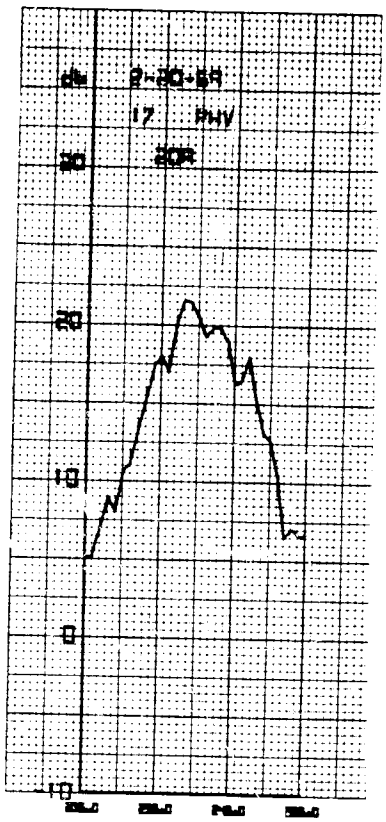
db 2-2C-69
17 PHV
2CR
30
20
10
0
-10

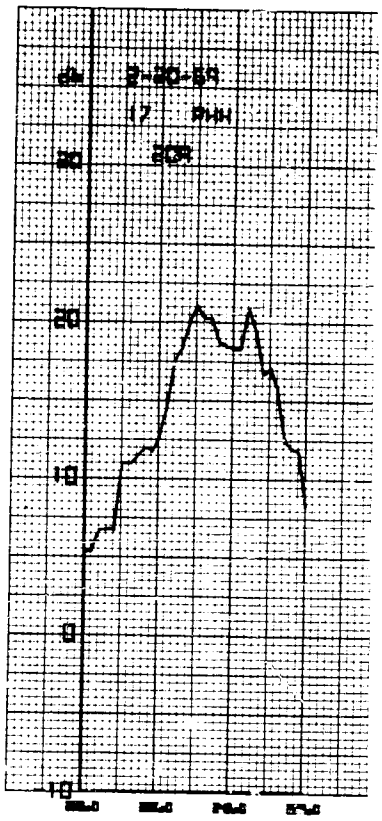
db 2-2C-69
17 PHH
2CR
30
20
10
0
-10

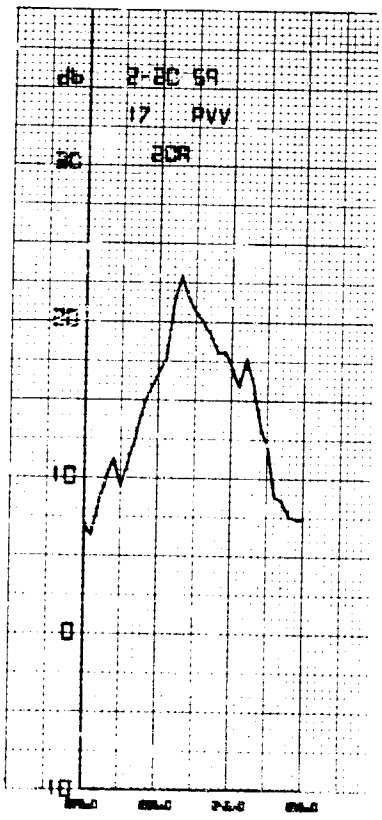
db 2-2C 69
17 PVV
2CR
30
20
10
0
-10

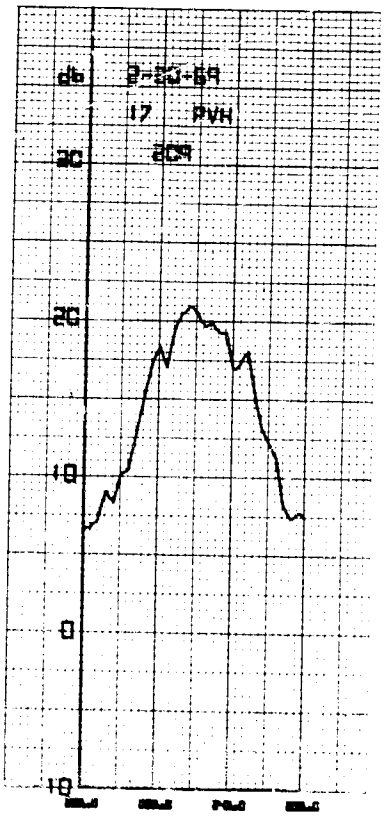
db 2-2C-69
17 PVH
2CR
30
20
10
0
-10

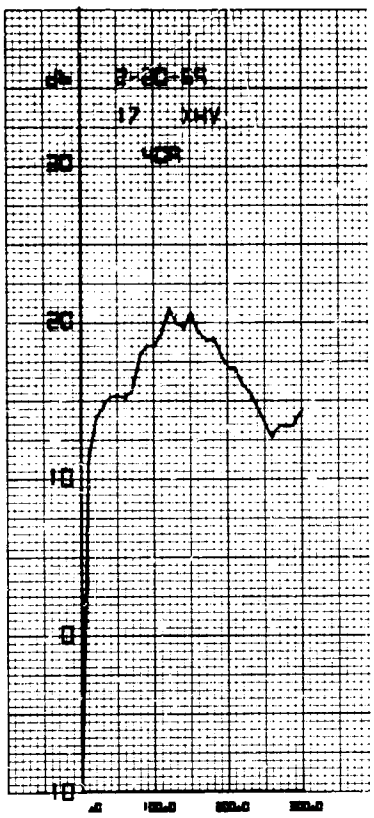
db
17 XHV
HDR
30
20
10
0
10

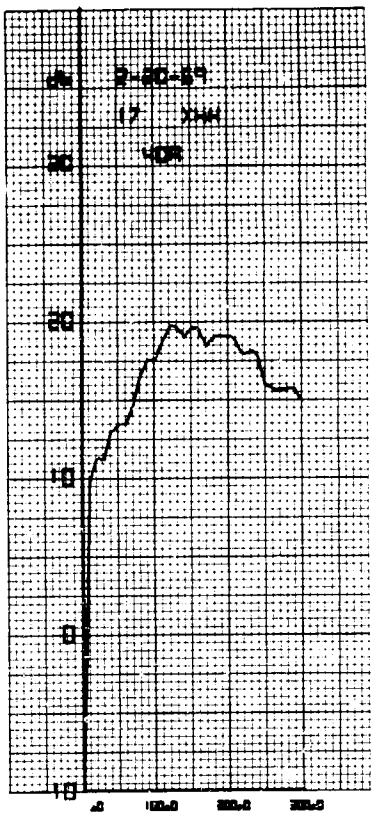
db
17 XHH
HDR
30
20
10
0
10

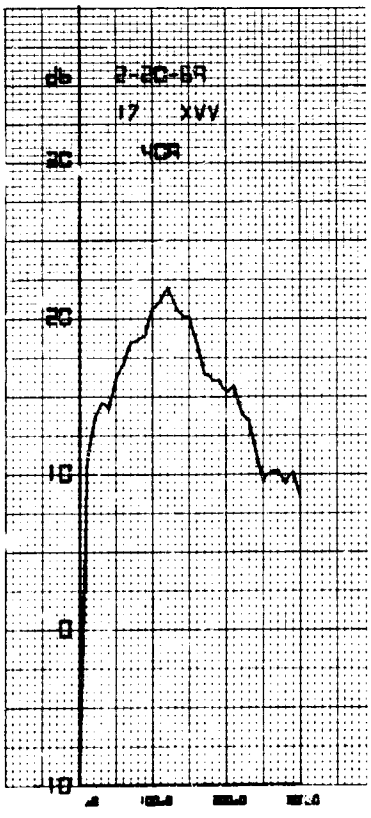
db
17 XVV
HDR
30
20
10
0
10

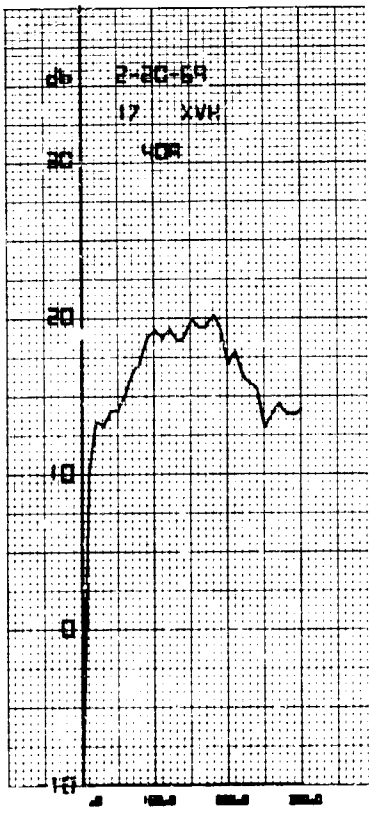
db
17 XVH
HDR
30
20
10
0
10

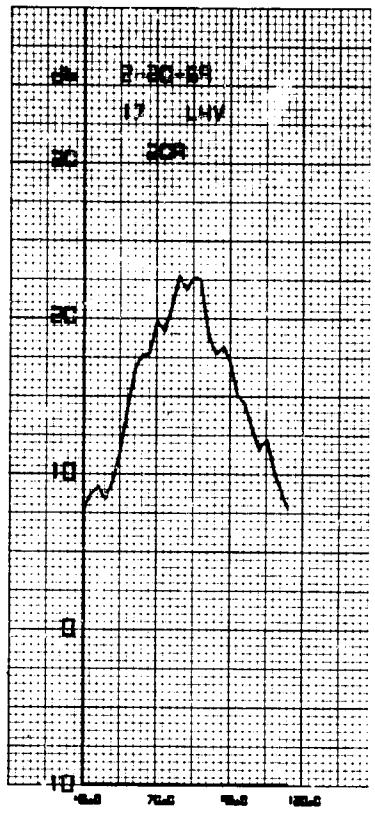
db
2-2C-69
17 LHV
20R
30
20
10
0
-10

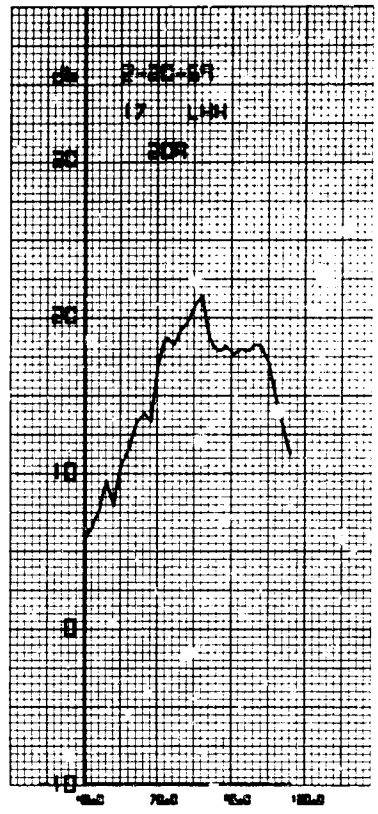
db
2-2C-69
17 LHH
20R
30
20
10
0
-10

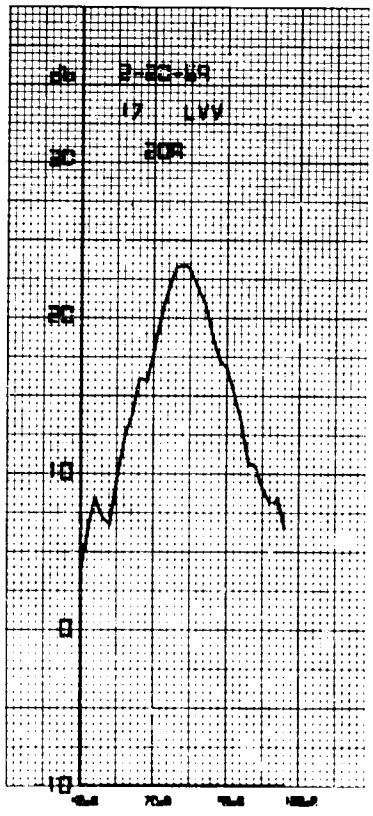
db
2-2C-69
17 LVV
20R
30
20
10
0
-10

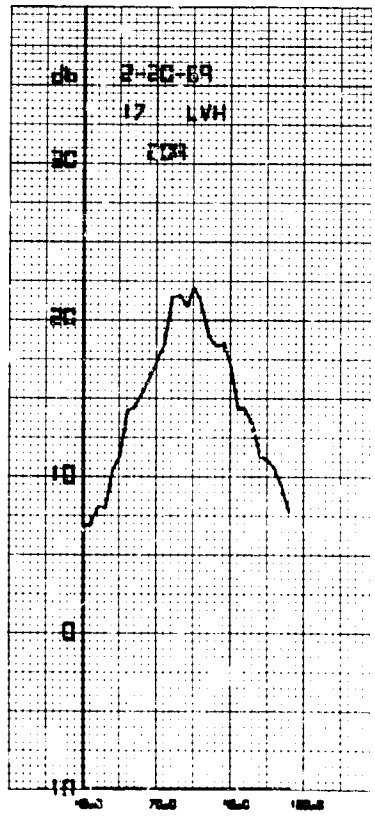
db
2-2C-69
17 LVH
20R
30
20
10
0
-10

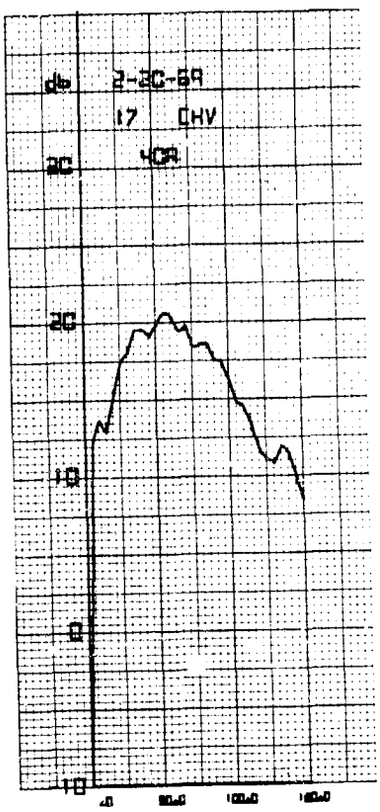
db 2-2C-89
17 CHV
4CR
30
20
10
0
-10

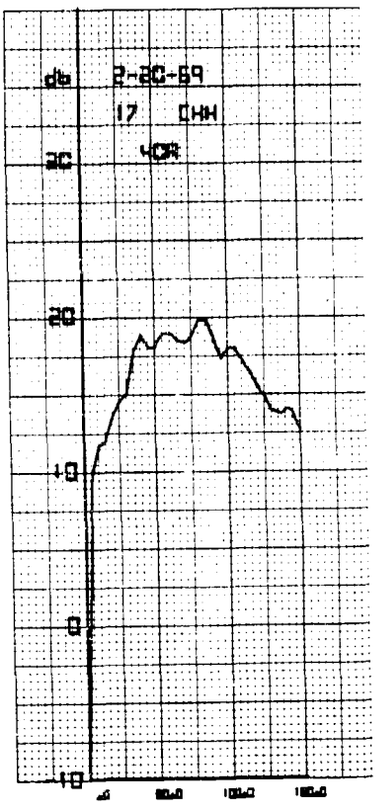
db 2-2C-89
17 CHH
4CR
30
20
10
0
-10

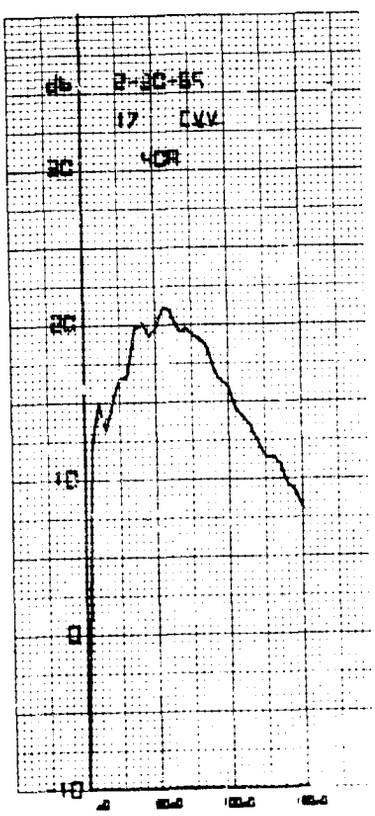
db 2-2C-85
17 CVV
4CR
30
20
10
0
-10

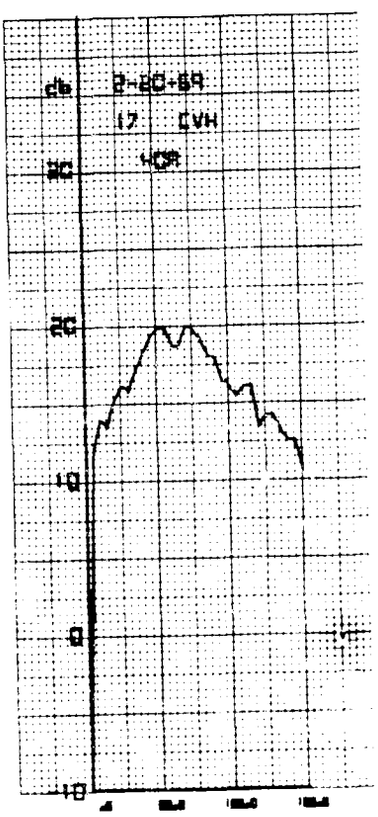
db 2-2C-89
17 CVH
4CR
30
20
10
0
-10

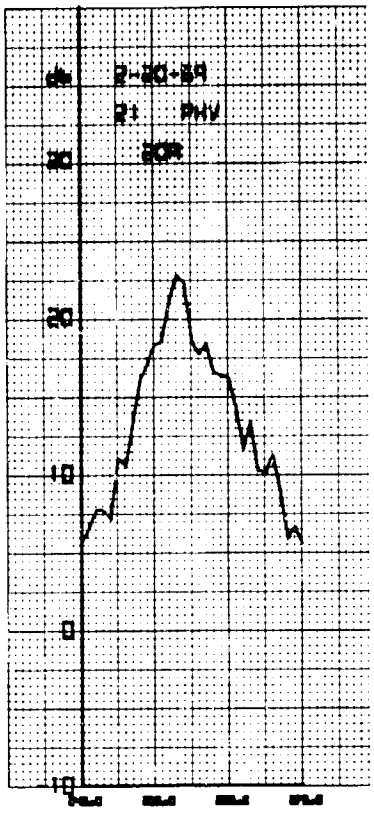

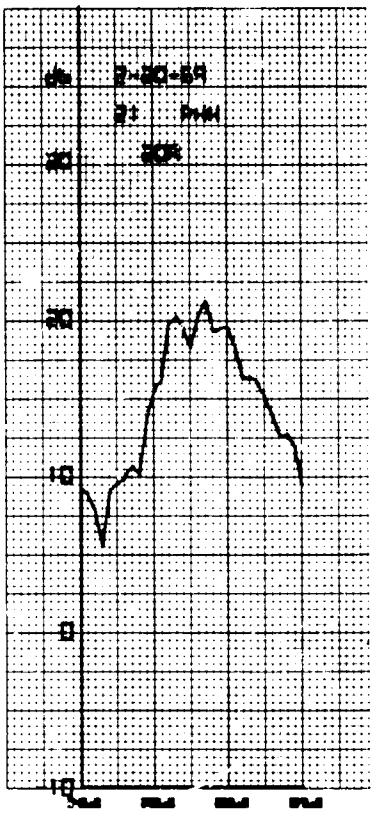

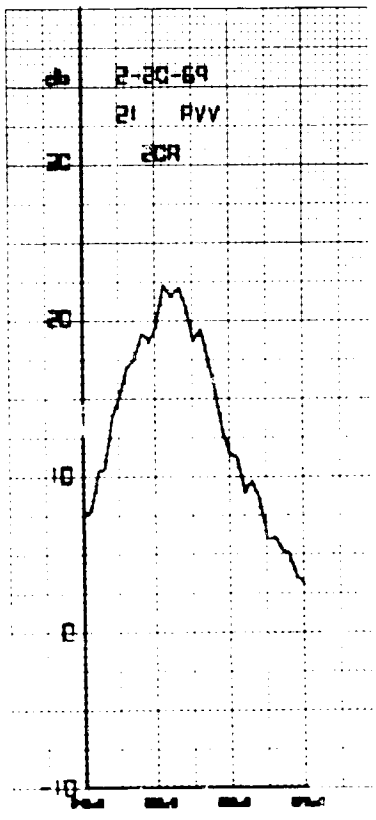

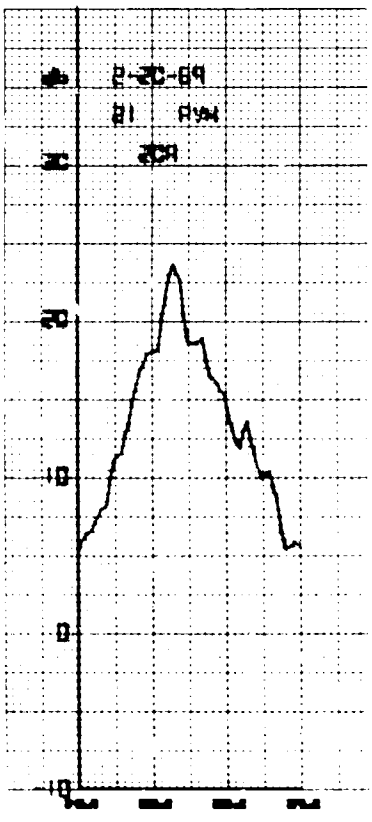

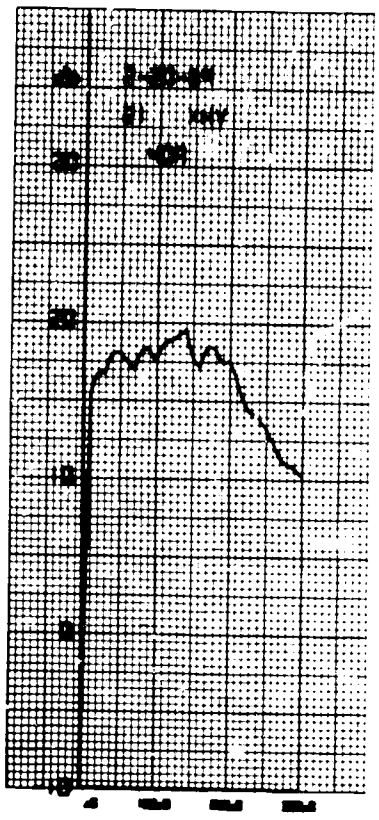

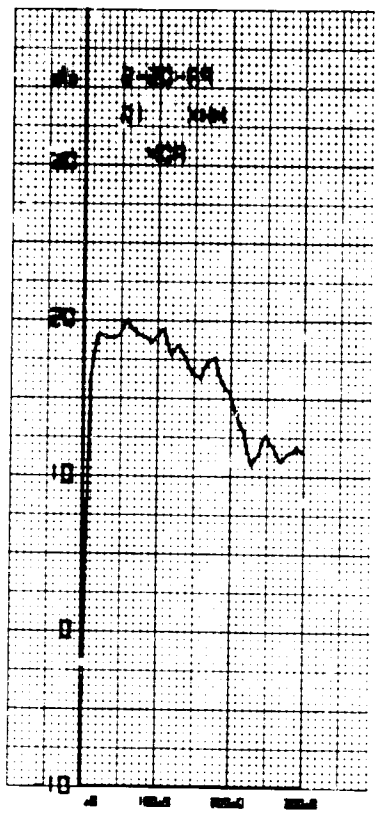

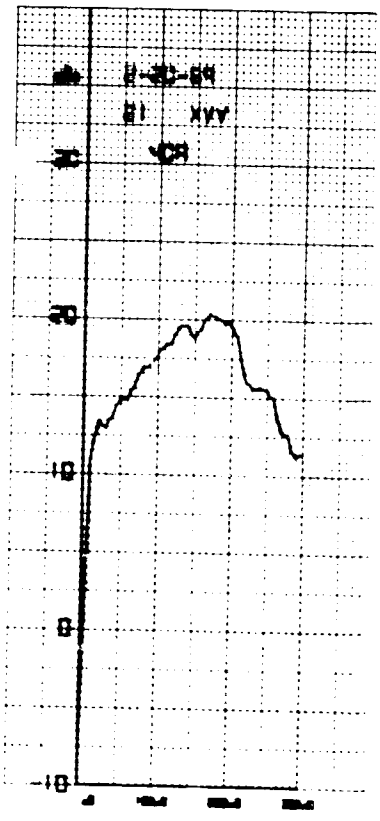

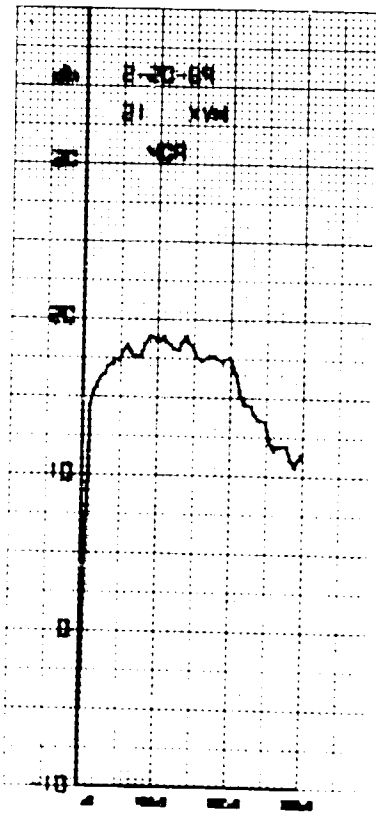

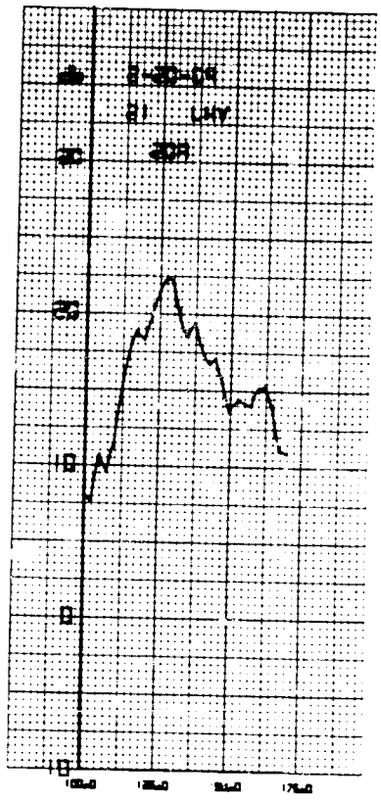

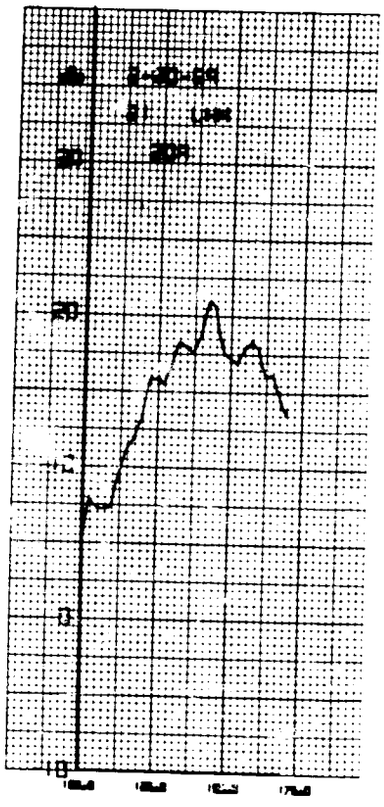

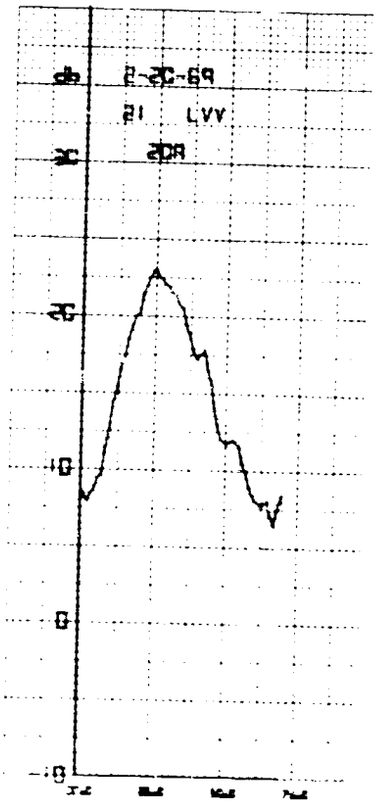

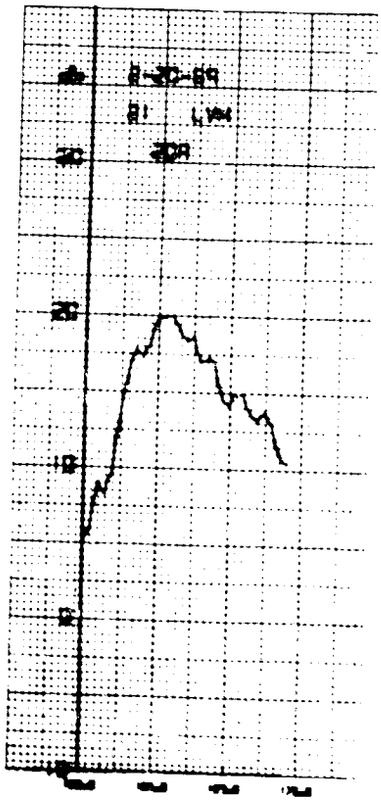

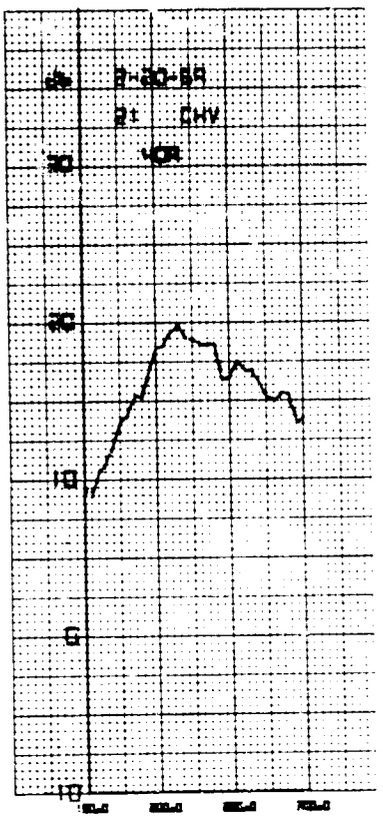

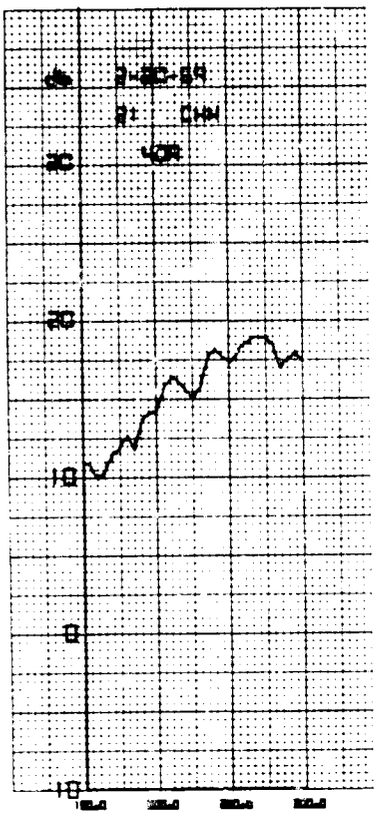

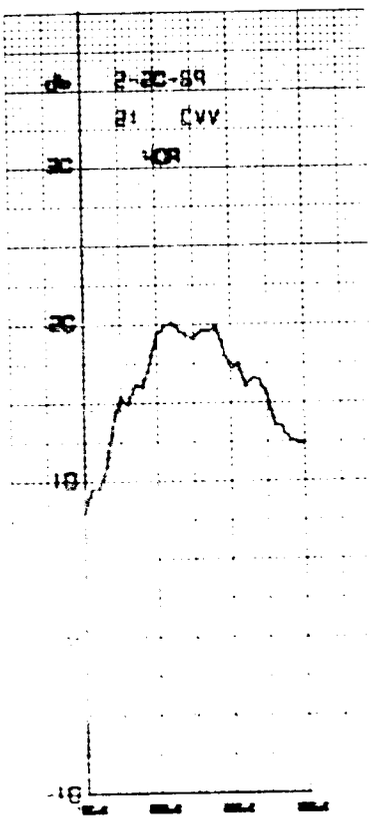

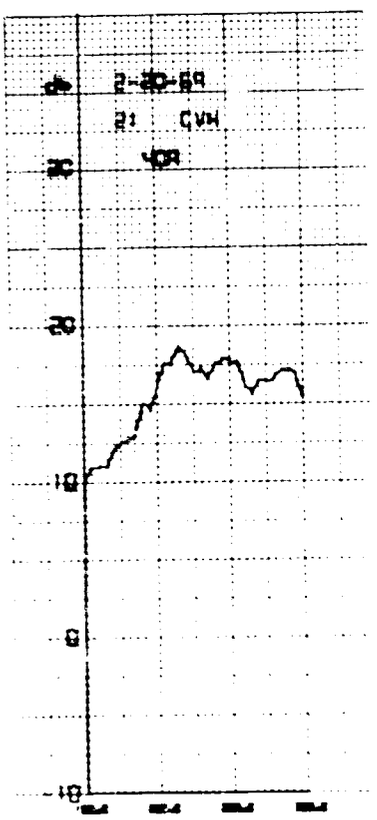

Security Classification

DOCUMENT CONTROL DATA - R & D

Security classification of title, body of abstract and indexing annotation must be entered when the overall report is classified)

1. ORIGINATING ACTIVITY (Corporate author)	2a. REPORT SECURITY CLASSIFICATION
Naval Research Laboratory Washington, D.C. 20390	Unclassified 2b. GROUP

3. REPORT TITLE

STUDY OF DOPPLER SPECTRA OF RADAR SEA-ECHO

4. DESCRIPTIVE NOTES *(Type of report and inclusive dates)*

An interim report on a continuing NRL Problem.

5. AUTHOR(S) *(First name, middle initial, last name)*

G.R. Valenzuela and M.B. Laing

6. REPORT DATE	7a. TOTAL NO. OF PAGES	7b. NO. OF REFS
November 3, 1969	56	20

8a. CONTRACT OR GRANT NO.	9a. ORIGINATOR'S REPORT NUMBER(S)
NRL Problem R02-37 b. PROJECT NO. A31-533/65269R008-01-02 c. d.	NRL Report 6934 9b. OTHER REPORT NO(S) *(Any other numbers that may be assigned this report)*

10. DISTRIBUTION STATEMENT

This document has been approved for public release and sale; its distribution is unlimited.

11. SUPPLEMENTARY NOTES	12. SPONSORING MILITARY ACTIVITY
	Department of the Navy (Naval Air Systems Command), Washington, D.C. 20360

13. ABSTRACT

Doppler spectra of radar sea-echo were investigated theoretically and experimentally. Electromagnetic scattering models were developed with composite rough surfaces, i.e., Bragg resonant water waves superimposed on a carrier water wave; and basic concepts in hydrodynamics were developed for a gravity wave of finite height. The ideas are carried over to the sea, where the assumption of a fully developed sea yields wave height expressions of the form $\sim H^{0.4 \text{ to } 0.6}$ for the width of the spectra of radar sea-echo, H being the height of the carrier water wave. The simple models yield the order of magnitude and the wave height dependence of the spectra width, but they fail to give its observed polarization dependence.

New experimental results on spectra of radar sea-echo from the Four-Frequency Radar (428 MHz, 1228 MHz, 4455 MHz, and 8910 MHz), for sea conditions which ranged from 1 to 2 ft waves and 1 to 2 knot winds to 26-ft waves and 46 to 48 knot winds, show that the bandwidth of radar sea-echo is polarization and frequency dependent, and the differential doppler, between horizontal and vertical polarization, is frequency and depression angle dependent. Both the "noisiness" of the spectra and the greater spectral width of the horizontal return indicate spray over the sea might be the mechanism responsible for the dependencies observed.

DD FORM 1 NOV 65 1473 (PAGE 1)

S/N 0101-807-6801

Security Classification

Security Classification

14 KEY WORDS	LINK A		LINK B		LINK C	
	ROLE	WT	ROLE	WT	ROLE	WT
Mathematical models						
Analysis (mathematical) (experimental)						
Sea clutter						
Doppler spectra						
Scattering model						
Multiple frequency radar						
Direct and crosspolarized echo						

DD FORM NO. 1473